Addition of Dimethyl Disulfide to 1. A mixture of **1** (1.20 g, 2.05 mmol), dimethyl disulfide (0.19 g, 2.05 mmol), and benzene (8 mL) was heated in a sealed tube at 80 °C for 4 h. After evaporation of the solvent at reduced pressure, the residue was recrystallized from pentane to afford 0.91 g of **24**: white crystals (yield 65%); mp 133-135 °C; ^{1}H NMR (C_6D_6) δ 1.40 (s, 9 H, *p*-*t*-Bu), 1.63 (s, 3 H, MeSGe), 1.77 (s, 18 H, *o*-*t*-Bu), 2.12 (s, 6 H, *p*-Me), 2.16 (d, ^3J(PH) = 12.7 Hz, 3 H, MeSP), 2.43 (s, 12 H, *o*-Me), 6.75 (s, 4 H, Ar Mes), 7.55 (d, ^4J(PH) = 2.6 Hz, 2 H, Ar Ar); ^{31}P{^{1}H} NMR (C_6D_6) δ 3.0. Anal. Calcd for $C_{38}H_{57}GePS_2$: C, 66.96; H, 8.43; S, 9.41. Found: C, 67.20; H, 8.58; S, 9.50.

Synthesis, Structure, and Spectroscopic Properties of Early Transition Metal η^2-Iminoacyl Complexes Containing Aryl Oxide Ligation

Linda R. Chamberlain,[†] Loren D. Durfee,[†] Phillip E. Fanwick,[†] Lisa Kobriger,[†] Stanley L. Latesky,[†] Anne K. McMullen,[†] Ian P. Rothwell,*[†1] Kirsten Folting,[‡] John C. Huffman,[‡] William E. Streib,[‡] and Ruji Wang[‡]

Contribution from the Department of Chemistry, Purdue University, West Lafayette, Indiana 47907, and the Molecular Structure Center, Indiana University, Bloomington, Indiana 47401. *Received July 22, 1986*

Abstract: A total of twenty η^2-iminoacyl derivatives of the metals titanium, zirconium, hafnium, and tantalum have been synthesized by the migratory insertion of organic isocyanides into the metal-alkyl bonds of a series of mixed alkyl, aryl oxide compounds. For the group 4 metals reaction of the bis-alkyls $(ArO)_2M(R)_2$ (M = Ti, Zr, Hf; ArO = 2,6-diisopropyl, 2,6-diphenyl, or 2,6-di-*tert*-butylphenoxide; R = CH_3, CH_2Ph, or CH_2SiMe_3) with R'NC leads initially to the mono-iminoacyl derivatives $(ArO)_2M(\eta^2\text{-R'NCR})(R)$ (I) and finally to the bis-insertion products $(ArO)_2M(\eta^2\text{-R'NCR})_2$ (II). The tris-benzyl complex $(2,6\text{-}t\text{-}Bu_2ArO)Zr(CH_2Ph)_3$ yields the complex $(2,6\text{-}t\text{-}Bu_2ArO)Zr(\eta^2\text{-R'NCCH}_2Ph)_3$ (IV) with 3 equiv of R'NC via the isolated bis-iminoacyl intermediate (III). For tantalum, the complex $Ta(OAr\text{-}2,6\text{-}Me_2)_3(\eta^2\text{-xyNCCH}_2Ph)_2$ (V) (OAr-2,6-Me_2 = 2,6-dimethylphenoxide) is readily formed from the corresponding bis-benzyl complex and 2 equiv of 2,6-dimethylphenyl isocyanide (xyNC). With the tris-alkyls $Ta(OAr\text{-}2,6\text{-}Me_2)_2(R)_3$ (R = CH_3, CH_2Ph), however, only 2 equiv of xyNC were found to insert readily leading to $Ta(OAr\text{-}2,6\text{-}Me_2)_2(\eta^2\text{-xyNCR})_2(R)$ (VI). The spectroscopic properties of all of these compounds is consistent with an η^2 coordination of the iminoacyl group. In order to confirm this and gain more insight into the structural parameters for this type of bonding, six single-crystal X-ray diffraction studies have been carried out on compounds of type I, II, IV, and VI. All compounds structurally characterized were found to have very similar M-N and M-C distances to the iminoacyl function with C-N distances being in the range 1.257 (6) to 1.285 (4) Å consistent with the presence of a double bond. Correlation of the observed solid-state structures of these complexes with their ^{1}H and ^{13}C NMR spectra indicate that the η^2-iminoacyl groups are fluxional. However, whether this fluxionality involves simple rotation while η^2 bound or an η^2-η^1-η^2 process could not be distinguished. The two mono-inserted compounds $Ti(OAr\text{-}2,6\text{-}i\text{-}Pr_2)_2(\eta^2\text{-}t\text{-BuNCCH}_2Ph)(CH_2Ph)$ (Ia) and $Ti(OAr\text{-}2,6\text{-}Ph_2)_2(\eta^2\text{-PhNCCH}_2SiMe_3)(CH_2SiMe_3)$ (Ib) adopt similar structures in which the η^2-iminoacyl and noninserted alkyl group are co-planar bisecting the plane of $(ArO)_2Ti$ unit with the carbon atoms mutually cis to each other. In the bis-iminoacyl derivatives $Zr(OAr\text{-}2,6\text{-}t\text{-}Bu_2)_2(\eta^2\text{-}t\text{-BuNCCH}_2Ph)_2$ (IId) and $Hf(OAr\text{-}2,6\text{-}t\text{-}Bu_2)_2(\eta^2\text{-PhNCMe})_2$ (IIg) the η^2-R'NCR units lie parallel to each other in a head-to-tail fashion, aligned approximately along the O-M-O plane. The tris-insertion complex $Zr(OAr\text{-}2,6\text{-}t\text{-}Bu_2)(\eta^2\text{-}t\text{-BuNCCH}_2Ph)_3$ (IVa) contains three nonequivalent η^2-iminoacyls arranged about the metal center. All three types of group 4 metal complexes I, II, and IV can best be described as containing a 4-coordinate environment about the metal in which each η^2-R'NCR group occupies a single coordination site. The compound $Ta(OAr\text{-}2,6\text{-}Me_2)_2(\eta^2\text{-xyNC-Me})_2(Me)$ (VIa) was found to contain the η^2-iminoacyl groups co-planar with mutually cis-carbon atoms. The metal coordination sphere could best be described as pentagonal bipyramidal with trans, axial aryl oxide groups. The summary of the crystal data is as follows: for $Ti(OAr\text{-}2,6\text{-}i\text{-}Pr_2)_2(\eta^2\text{-}t\text{-BuNCCH}_2Ph)(CH_2Ph)$ (Ia) at -154 °C, a = 18.678 (7) Å, b = 11.724 (4) Å, c = 9.053 (3) Å, α = 111.99 (2), β = 74.23 (2)°, γ = 101.96 (2)°, Z = 2, d_{calcd} = 1.148 g cm^{-3} in space group $P\bar{1}$; for $Ti(OAr\text{-}2,6\text{-}Ph_2)_2(\eta^2\text{-PhNCCH}_2SiMe_3)(CH_2SiMe_3)$ (Ib) at -160 °C, a = 23.086 (9) Å, b = 11.100 (4) Å, c = 10.122 (3) Å, α = 95.94 (2)°, β = 107.38 (2)°, γ = 78.51 (2)°, Z = 2, d_{calcd} = 1.178 g cm^{-3} in space group $P\bar{1}$; for $Zr(OAr\text{-}2,6\text{-}t\text{-}Bu_2)_2(\eta^2\text{-}t\text{-BuNCCH}_2Ph)_2$ (IId) at -157 °C, a = 23.612 (8) Å, b = 11.198 (4) Å, c = 21.243 (8) Å, β = 123.52 (2)°, Z = 4, d_{calcd} = 1.206 g cm^{-3} in space group $C2/c$; for $Hf(OAr\text{-}2,6\text{-}t\text{-}Bu_2)_2(\eta^2\text{-PhNCMe})_2$ (IIg) at 22 °C, a = 13.203 (3) Å, b = 15.150 (3) Å, c = 21.213 (6) Å, β = 103.33 (2)°, Z = 4, d_{calcd} = 1.328 g cm^{-3} in space group $C2/c$; for $Zr(OAr\text{-}2,6\text{-}t\text{-}Bu_2)(\eta^2\text{-}t\text{-BuNCCH}_2Ph)_3$ (IVa) at -155 °C, a = 14.031 (5) Å, b = 15.788 (7) Å, c = 10.918 (4) Å, α = 108.89 (2)°, β = 97.01 (2)°, γ = 94.30 (2)°, Z = 2, d_{calcd} = 1.207 g cm^{-3} in space group $P\bar{1}$; for $Ta(OAr\text{-}2,6\text{-}Me_2)_2(\eta^2\text{-xyNCMe})_2(Me)$ (VIa) at -160 °C, a = 10.881 (2) Å, b = 18.154 (5) Å, c = 9.188 (2) Å, α = 99.07 (1)°, β = 108.80 (1)°, γ = 75.36 (1)°, Z = 2, d_{calcd} = 1.465 g cm^{-3} in space group $P\bar{1}$.

The migratory insertion of carbon monoxide into metal-carbon bonds is an organometallic reaction that has deservedly received considerable study.[2] However, it is the structure and reactivity of the ensuing metal-acyl functional group that determines the organic products that one might expect from transition metal mediated utilization of CO.[3] For high valent, electron deficient (oxophilic) metals such as the early d-block,[4-6] lanthanides and[7]

[†] Purdue University.
[‡] Indiana University.

(1) (a) Camille and Henry Dreyfus Teacher-Scholar, 1985-1990. (b) Fellow of the Alfred P. Sloan Foundation, 1986-1990.
(2) (a) Calderazzo, F. *Angew. Chem., Int. Ed. Engl.* **1977**, *16*, 299. (b) Kuhlmann, K. J.; Alexander, J. J. *Coord. Chem. Rev.* **1980**, *33*, 195. (c) Wojcicki, A. *Adv. Organomet. Chem.* **1973**, *11*, 87.

0002-7863/87/1509-0390$01.50/0

Scheme I

$$(ArO)_2M(R)_2 \xrightarrow{R'NC} (ArO)_2M(\eta^2\text{-}R'NCR)(R) \xrightarrow{R'NC} (ArO)_2M(\eta^2\text{-}R'NCR)_2$$
(I) (II)

	M	ArO	R	R'
Ia	Ti	OAr-2,6Pr$^i_2$	CH_2Ph	Bu^t
Ib	Ti	OAr-2,6Ph$_2$	CH_2SiMe_3	Ph
Ic	Ti	OAr-2,6Ph$_2$	CH_2SiMe_3	xy
Id	Ti	OAr-2,6Ph$_2$	CH_2Ph	xy
Ie	Zr	OAr-2,6Bu$^t_2$	CH_2Ph	xy
IIa	Ti	OAr-2,6Pr$^i_2$	CH_2Ph	xy
IIb	Ti	OAr-2,6Ph$_2$	CH_2Ph	xy
IIc	Zr	OAr-2,6Bu$^t_2$	CH_2Ph	xy
IId	Zr	OAr-2,6Bu$^t_2$	CH_2Ph	Bu^t
IIe	Zr	OAr-2,6Bu$^t_2$	CH_3	xy
IIf	Zr	OAr-2,6Bu$^t_2$	CH_3	Ph
IIg	Hf	OAr-2,6Bu$^t_2$	CH_3	Ph

actinides,[8] the resulting acyl (and related formyl) group typically adopts a η^2 bound structure involving coordination through both oxygen and carbon atoms. The structural and spectroscopic properties and particularly the reactivity of these η^2-acyls and formyls has led to the proposal that a significant amount of oxy–carbene resonance exists for the ligand.[4a,9-11] Of particular importance is their demonstrated ability to undergo both inter- and intramolecular coupling to produce cis and trans ene-diolates,[10,12] reduction by metal hydrides to produce alkoxides,[4a,13] and ability to undergo further reaction with CO to produce dionediolate ligands.[7b,8a] In contrast to the extensive studies reported on the spectroscopic and structural properties of the η^2-acyl function, the study of the isoelectronic η^2-iminoacyl ligand formed by the migratory insertion of organic isocyanides (RNC) into metal alkyl bonds is much less thorough.[14-20] We wish to report here a combination of synthetic, spectroscopic, and structural studies on a number of early transition metal aryl oxide compounds containing η^2-iminoacyl ligands. This work has allowed us to isolate and study compounds containing more than one η^2-iminoacyl function, a situation as yet unknown for their η^2-acyl counterparts.[21] Compounds such as these are of importance as they may give insights into the pathways whereby the observed intramolecular coupling (carbon–carbon double bond formation) of these types of ligand can take place to produce ene-diolate, enamidolate, or ene-diamide functional groups.[22]

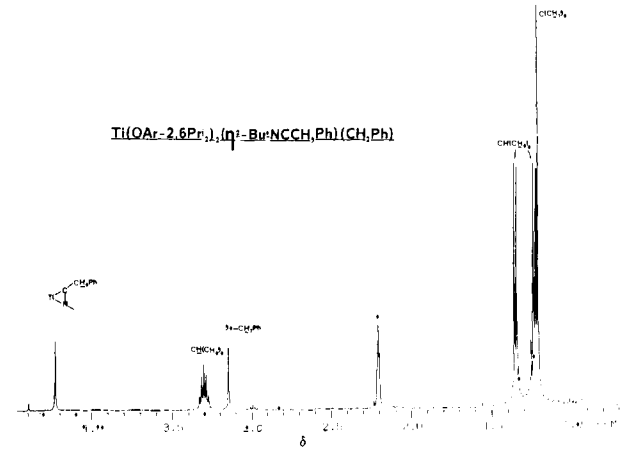

Figure 1. ^1H NMR spectrum of Ti(OAr-2,6-*i*-Pr_2)$_2$(η^2-*t*-BuNCCH$_2$Ph)(CH$_2$Ph) (Ia) showing the diastereotopic isopropyl methyl groups. The protio impurity in the toluene-d_8 solvent is indicated by an asterisk.

Scheme II

$$(ArO)Zr(\eta^2\text{-}R'NCCH_2Ph)_2(CH_2Ph) \text{ (III)}$$
$$(ArO)Zr(CH_2Ph)_3 \xrightarrow{3R'NC} (ArO)Zr(\eta^2\text{-}R'NCCH_2Ph)_3 \text{ (IV)}$$

ArO = OAr-2,6Bu$^t_2$

(III): R' = xy; (IVa): R' = Bu^t; (IVb): R' = xy.

Scheme III

$$(ArO)_2Ta(CH_2Ph)_3 \xrightarrow{2xyNC} (ArO)_2Ta(\eta^2\text{-}xyNCCH_2Ph)_2 \text{ (V)}$$
$$(ArO)_2Ta(R)_3 \xrightarrow{2R'NC} (ArO)_2Ta(\eta^2\text{-}R'NCR)_2(R) \text{ (VI)}$$

ArO = OAr-2,6Me$_2$

(VIa): R = CH_2, R' = xy; (VIb): R = CH_2, R' = iso; (VIc): R = CH_2Ph, R' = xy; (VId): R = CH_2Ph, R' = iso.

(3) Ford, P. C., Ed. *Catalytic Activation of Carbon Monoxide*; ACS Symposium Series 152; American Chemical Society: Washington, Dc., 1981.

(4) (a) Wolczanski, P. T.; Bercaw, J. E. *Acc. Chem. Res.* **1980**, *13*, 121. (b) Erker, G. *Acc. Chem. Res.* **1984**, *17*, 103.

(5) (a) Fachinetti, G.; Fochi, G.; Floriani, C. *J. Chem. Soc., Dalton Trans.* **1977**, 1946. (b) Fachinetti, G.; Floriani, C.; Stoeckli-Evans, H. *J. Chem. Soc., Dalton Trans.* **1977**, 2297.

(6) Curtis, M. D.; Shiu, K. B.; Butler, W. M. *J. Am. Chem. Soc.*, in press, and references therein.

(7) (a) Evans, W. J. *Adv. Organomet. Chem.* **1985**, *24*, 131. (b) Evans, W. J.; Wayda, A. L.; Hunter, W. E.; Atwood, J. L. *J. Chem. Soc., Chem. Commun.* **1981**, 706.

(8) (a) Moloy, K. G.; Fagan, P. J.; Manriquez, J. M.; Marks, T. J. *J. Am. Chem. Soc.* **1986**, *108*, 56. (b) Marks, T. J. *Science* **1982**, *217*, 989. (c) Moloy, K. G.; Marks, T. J. *J. Am. Chem. Soc.* **1984**, *106*, 7051. (d) Maata, E. A.; Marks, T. J. *J. Am. Chem. Soc.* **1981**, *103*, 3576.

(9) Manriquez, J. M.; McAlister, D. R.; Sanner, R. D.; Bercaw, J. E. *J. Am. Chem. Soc.* **1976**, *98*, 6733.

(10) Marks, T. J.; Day, V. W. In *Fundamental and Technological Aspects of Organo-f-Element Chemistry*; Marks, T. J., Fragala, I. L., Eds.; Dordrecht: Holland, 1986.

(11) Theoretical studies of the bonding of η^2-acyl groups have been carried out, see: (a) Tatsumi, K.; Nakamura, A.; Hofmann, P.; Stauffert, P.; Hoffman, R. *J. Am. Chem. Soc.* **1985**, *107*, 4440. Tatsumi, K.; Nakamura, A.; Hoffmann, R. *Organometallics* **1985**, *4*, 404.

(12) (a) Manriquez, J. M.; McAlister, D. R.; Sanner, R. D.; Bercaw, J. E. *J. Am. Chem. Soc.* **1978**, *100*, 2716. (b) McDade, C.; Bercaw, J. E. *J. Organomet. Chem.* **1985**, *279*, 281. (c) Gambarotta, S.; Floriani, C.; Chiesi-Villa, A.; Guastini, C. *J. Am. Chem. Soc.* **1983**, *105*, 1690. (d) Evans, W. J.; Grate, J. W.; Doedens, R. J. *J. Am. Chem. Soc.* **1985**, *107*, 1671.

(13) (a) Maata, E. A.; Marks, T. J. *J. Am. Chem. Soc.* **1981**, *103*, 3576. (b) Marsella, J.; Folting, K.; Huffman, J. C.; Caulton, K. G. *J. Am. Chem. Soc.* **1981**, *103*, 5596. (c) Wolczanski, P. T.; Threlkel, R. S.; Bercaw, J. E. *J. Am. Chem. Soc.* **1979**, *101*, 218. (d) Gell, K. I.; Posin, G.; Schwartz, J.; Williams, G. M. *J. Am. Chem. Soc.* **1982**, *104*, 1846.

(14) (a) Treichel, P. M. *Adv. Organomet. Chem.* **1983**, *11*, 21 and references therein. (b) Singleton, E.; Oosthuizen, H. E. *Adv. Organomet. Chem.* **1983**, *22*, 209.

(15) (a) Chiu, K. W.; Jones, R. D.; Wilkinson, G.; Galas, A. M. R.; Hursthouse, M. B. *J. Chem. Soc., Dalton Trans.* **1981**, 2088. (b) Andersen, R. A. *Inorg. Chem.* **1979**, *18*, 2928. (c) Curtis, M. D., private communication.

(16) (a) Klei, K.; Telgen, J. H.; Teuben, J. H. *J. Organomet. Chem.* **1981**, *209*, 297. (b) Bolhuis, F.; DeBoer, K. J. M.; Teuben, J. H. *J. Organomet. Chem.* **1979**, *170*, 299. (c) Lappert, M. F.; Luong-Thi, N. T.; Milne, C. R. C., *J. Organomet. Chem.* **1979**, *174*, C35.

(17) (a) Wolczanski, P. T.; Bercaw, J. E.; *J. Am. Chem. Soc.*, **1979**, *101*, 6450. (b) Evans, W. J.; Meadows, J. H.; Hunton, W. R.; Atwood, J. L. *Organometallics* **1983**, *2*, 1252.

(18) (a) Zarella, P.; Paducci, G.; Rossetto, G.; Beretollo, F.; Po, D.; Fischer, R. D.; Bombien, G. *J. Chem. Soc., Chem. Commun.* **1985**, 96. (b) Reger, D. L.; Targuini, M. K.; Lebiodra, L. *Organometallics* **1983**, *2*, 1763.

(19) (a) Adams, R. D.; Chodosh, D. F. *Inorg. Chem.* **1978**, *17*, 41. (b) Adams, R. D.; Golembeski, N. M. *Inorg. Chem.* **1978**, *17*, 1969. (c) Adams, R. D.; Golembeski, N. M. *J. Am. Chem. Soc.* **1979**, *101*, 2579.

(20) (a) Mays, M. J.; Prost, D. W.; Raithby, P. R. *J. Chem. Soc., Chem. Commun.* **1980**, 171. (b) Andrews, M. A.; VanBuskirk, G.; Knobler, C. D.; Kaesz, H. D. *J. Am. Chem. Soc.* **1979**, *101*, 7245. (c) Christian, D. F.; Clark, G. R.; Royer, W. R.; Waters, J. M.; Whittle, K. R. *J. Chem. Soc., Chem. Commun.* **1972**, 458. (d) Clark, G. R.; Waters, J. M.; Whittle, K. R. *J. Chem. Soc., Dalton Trans.* **1975**, 2556. (e) Christian, D. F.; Clark, H. C.; Stepaniak, R. F. *J. Organomet. Chem.* **1976**, *112*, 209.

(21) The bis-insertion of CO into the metal–nitrogen bonds of $Cp_2M(NMe_2)_2$ (M = μ, Th) to produce a bis-imidoyl complex; see: Fagan, P. J.; Manriquez, J. M.; Vollmer, S. H.; Day, C. S.; Day, V. W.; Marks, T. J. *J. Am. Chem. Soc.* **1981**, *103*, 2206.

(22) Some aspects of this work have been communicated: (a) McMullen, A. K.; Rothwell, I. P.; Huffman, J. C. *J. Am. Chem. Soc.* **1985**, *107*, 1072. (b) Latesky, S. L.; McMullen, A. K.; Rothwell, I. P.; Huffman, J. C. *Organometallics* **1985**, *4*, 1986. (c) Chamberlain, L. R.; Rothwell, I. P.; Huffman, J. C. *J. Chem. Soc., Chem. Commun.* **1986**, 1203.

Table I. Selected Spectroscopic Data

complex	δ(R′NCR)[a]	$\bar{\nu}$(C=N)[b]
Ti(OAr-2,6-*i*-Pr$_2$)$_2$(η^2-*t*-BuNCCH$_2$Ph)(CH$_2$Ph) (Ia)	230.5	1560
Ti(OAr-2,6-Ph$_2$)$_2$(η^2-PhNCCH$_2$SiMe$_3$)(CH$_2$SiMe$_3$) (Ib)	240.7	1565
Ti(OAr-2,6-Ph$_2$)$_2$(η^2-xyNCCH$_2$SiMe$_3$)(CH$_2$SiMe$_3$) (Ic)	242.4	1560
Ti(OAr-2,6-Ph$_2$)$_2$(η^2-xyNCCH$_2$Ph)(CH$_2$Ph) (Id)	238.9	1595
Zr(OAr-2,6-*t*-Bu$_2$)$_2$(η^2-xyNCCH$_2$Ph)(CH$_2$Ph) (Ie)	246.3	1530
Ti(OAr-2,6-*i*-Pr$_2$)$_2$(η^2-xyNCCH$_2$Ph)$_2$ (IIa)	237.1	1580
Ti(OAr-2,6-Ph$_2$)$_2$(η^2-xyNCCH$_2$Ph)$_2$ (IIb)	241.1	1587
Zr(OAr-2,6-*t*-Bu$_2$)$_2$(η^2-xyNCCH$_2$Ph)$_2$ (IIc)	239.0	1560
Zr(OAr-2,6-*t*-Bu$_2$)$_2$(η^2-*t*-BuNCCH$_2$Ph)$_2$ (IId)	244.3	1570
Zr(OAr-2,6-*t*-Bu$_2$)$_2$(η^2-xyNCCH$_3$)$_2$ (IIe)	245.2	1579
Zr(OAr-2,6-*t*-Bu$_2$)$_2$(η^2-PhNCCH$_3$)$_2$ (IIf)	236.4	1560
Hf(OAr-2,6-*t*-Bu$_2$)$_2$(η^2-PhNCCH$_3$)$_2$ (IIg)	255.0	1550
Zr(OAr-2,6-bu$_2$)(η^2-*t*-BuNCCH$_2$Ph)$_3$ (IVa)	256.6	1560
Zr(OAr-2,6-*t*-Bu$_2$)(η^2-xyNCCH$_2$Ph)$_3$ (IVb)	247.1, 262.3[c]	1580
Ta(OAr-2,6-Me$_2$)$_3$(η^2-xyNCCH$_2$Ph)$_2$ (V)	241.7	1568
Ta(OAr-2,6-Me$_2$)$_2$(η^2-xyNCCH$_3$)$_2$(CH$_3$) (VIa)	239.6	1590
Ta(OAr-2,6-Me$_2$)$_2$(η^2-isoNCCH$_3$)$_2$(CH$_3$) (VIb)	240.8	1585
Ta(OAr-2,6-Me$_2$)$_2$(η^2-xyNCCH$_2$Ph)$_2$(CH$_2$Ph) (VIc)	239.7	1580
Ta(OAr-2,6-Me$_2$)$_2$(η^2-isoNCCH$_2$Ph)$_2$(CH$_2$Ph) (VId)	240.1	1590

[a] Recorded in C_6D_6 at 30 °C unless otherwise stated. [b] Nujol mull between KBr plates. [c] At −60 °C in toluene-d_8.

Results and Discussion

Synthesis of Complexes. Our studies of early transition metal aryloxide chemistry have made available to us a series of group 4 and group 5 metal compounds containing a combination of aryl oxide ligands and alkyl functional groups.[23] We have investigated the reactivity of some of these compounds toward a number of alkyl and aryl isocyanides. The products of these reactions are categorized depending on the stoichiometry M(OAr)$_x$(R)$_y$ of the initial alkyl substrate.

Bis-Alkyls M(OAr)$_2$R$_2$ (M = Ti, Zr, Hf). Five alkyl substrates of this stoichiometry containing the ligands 2,6-di-*tert*-butyl (OAr-2,6-*t*-Bu$_2$), 2,6-diisopropyl (OAr-2,6-*i*-Pr$_2$), or 2,6-diphenylphenoxide (OAr-2,6-Ph$_2$) were investigated, and the results are collected in Scheme I. All of the alkyls react smoothly with alkyl or aryl isocyanide in hydrocarbon solvents to give the mono- and bis-insertion products I and II sequentially. The intermediate I was detected spectroscopically (^{1}H NMR) in all cases when <2 equiv of isocyanide was added. However, isolation of pure I was only possible in a number of cases. The yield of the bis-iminoacyl compounds II was quantitative by ^{1}H NMR when sufficient isocyanide reagent was used. All of the products in Scheme I exhibit high solubility in aromatic hydrocarbons but lower solubility in pentane or hexane from which they can typically be recrystallized on cooling.

Zr(OAr-2,6-*t*-Bu$_2$)(CH$_2$Ph)$_3$. This tris-benzyl compound will react with ≥3 equiv of *t*-BuNC or 2,6-dimethylphenyl isocyanide (xyNC) in hexane or benzene solvent to give a high yield of the corresponding tris-iminoacyl complexes (IV) as shown (Scheme II). However, the intermediate bis-iminoacyl (III) could also be isolated when 2 equiv of xyNC were used, although unlike the previous derivatives, III was found to be thermally unstable at room temperature over a period of days.

Ta(OAr-2,6-Me$_2$)$_3$(CH$_2$Ph)$_2$. The colorless bis-benzyl complex Ta(OAr-2,6-Me$_2$)$_3$(CH$_2$Ph)$_2$ reacts rapidly with ≥2 equiv of 2,6-dimethylphenyl isocyanide (xyNC) in hexane to give a yellow microcrystalline precipitate of the sparingly soluble bis-insertion product V (Scheme III). The complex can be readily recrystallized from toluene solutions on cooling.

Tris-Alkyls Ta(OAr-2,6-Me$_2$)$_2$(R)$_3$ (R = CH$_3$, CH$_2$Ph). These colorless tris-alkyls of tantalum react with ≥2 equiv of 2,6-dimethylphenyl (xyNC) or 2,6-diisopropylphenyl isocyanide (isoNC) to produce the bis-iminoacyl complexes VI as shown (Scheme III). The products are formed in high yield and can be readily recrystallized from hexane–toluene mixtures. The products obtained from the trimethyl complex, VIa and VIb, are stable for hours in solution at 25 °C. However, over days the solutions become deep-purple with formation of a new complex in almost quantitative yield as judged by ^{1}H NMR studies. The benzyl complexes are thermally much more robust, being stable for months in solution.

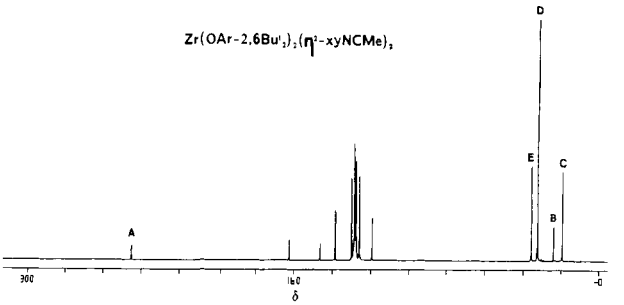

Figure 2. ^{13}C NMR spectrum of Zr(OAr-2,6-*t*-Bu$_2$)$_2$(η^2-xyNCMe)$_2$ (IIe). Assignments are the following: A, xyN*C*Me; B, xyNC*Me*; C, xy-*CH*$_3$; D and E, OAr-2,6-*t*-*Bu*$_2$.

Spectroscopic Properties of the η^2-Iminoacyl Groups. We believe all of the compounds prepared in this study contain the iminoacyl function both carbon and nitrogen bound in an η^2-fashion. This is based on the observed solid-state structure of six of the derivatives (vide infra) combined with the similarity of their spectroscopic properties (Table I). In the ^{1}H NMR spectra, the insertion of the alkyl or aryl isocyanide into the metal–alkyl bond was found to result in a downfield shift of the α-hydrogens attached to the initial alkyl carbon. Hence in the mono-inserted complex Ti(OAr-2,6-Ph$_2$)$_2$(CH$_2$Ph)(η^2-xyNCCH$_2$Ph) (Id) the two singlets at δ 3.05 and 2.01 are assignable to the methylene protons of the inserted and noninserted benzyl groups (see also Figure 1). In contrast the ^{13}C NMR resonance of the alkyl α-carbon shifts dramatically upfield on insertion, compare values of δ 41.7 and 76.3 for the inserted and noninserted benzyl groups of Id above.

The most notable characteristic of the NMR spectra of the η^2-iminoacyl complexes is the position of the resonance for the η^2-R′N*C*R carbon atom (Table I). For all of the complexes obtained in this study, this carbon was found to resonate between δ 230 and 265 (Figure 2). The shifting to lower field of the carbon resonance of acyl ligands has been shown to be characteristic of η^2-coordination,[6] and the magnitude of the downfield shift has been correlated with the contribution of the oxy–carbene resonance to the structure.[8a] Also, it has been shown by Adams that the iminoacyl carbon in the complex CpMo(CO)$_2$(η^2-CH$_3$CNCH$_3$)

(23) (a) Latesky, S. L.; McMullen, A. K.; Niccolai, G. P.; Rothwell, I. P.; Huffman, J. C. *Organometallics* **1985**, *4*, 902. (b) Latesky, S. L.; McMullen, A. K.; Rothwell, I. P.; Huffman, J. C. *J. Am. Chem. Soc.* **1985**, *107*, 5981. (c) Chamberlain, L. R.; Rothwell, I. P.; Huffman, J. C. *J. Chem. Soc., Dalton, Trans.*, in press. (d) Durfee, L. D.; Kobriger, L.; Rothwell, I. P., results to be published.

(24) Theoretical studies indicate that for the group 4 metals a ground state $\eta^2 + \eta^1$ coordination mode would be adopted for these molecules: Tatsumi, K.; Nakamura, A.; Hofman, P.; Hoffmann, R.; Moloy, K. G.; Marks, T. J. *J. Am. Chem. Soc.* **1986**, *108*, 4467.

Chart I

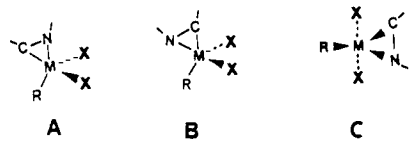

resonates approximately 40 ppm downfield of the corresponding resonance in $CpMo(CO)_2(P(OMe)_3)(\eta^1\text{-}CH_3CNPh)$.[19a] The chemical shift values obtained in this present study compare well with those previously reported for other η^2-iminoacyl derivatives of these metals.[14-20]

Another important spectroscopic characteristic of early transition metal, actinide and lanthanide η^2-acyl complexes is the low value of $\bar{\nu}$(CO) typically found.[4,5,8] In the case of actinide systems studied by Marks this vibration comes as low as 1452 cm^{-1}.[10] However, in the case of iminoacyl ligands the value of $\bar{\nu}$(CN) has been found to be a poor and somewhat inconsistent parameter for the assignment of the bonding mode.[16] The frequency of $\bar{\nu}$(CN) for η^1-iminoacyl groups bound to electron rich, later transition metal systems typically lies in the 1580–1680-cm^{-1} range. However, in the molybdenum systems mentioned earlier the change to an η^2-mode of bonding was found to give rise to an *increase* in $\bar{\nu}$(CN) to the 1680–1720-cm^{-1} region.[19a] For our compounds we find $\bar{\nu}$(CN) for the η^2-iminoacyl groups to lie in the region 1520–1590 cm^{-1} (Table I). This is comparable to values reported in the literature for this group bound to related early transition metal centers.[15b,16c,18b]

Solid-State and Solution Structures. In order to gain more insight into the structural aspects of the η^2-coordination of the iminoacyl group as well as information concerning the stereochemistry of metal complexes containing these ligands, six X-ray diffraction studies were carried out on a representative number of compounds. These will be discussed along with the solution NMR studies of the complexes in order to correlate the coordination environment and fluxionality of these molecules.

$Ti(OAr\text{-}2,6\text{-}i\text{-}Pr_2)_2(CH_2Ph)(\eta^2\text{-}t\text{-}BuNCCH_2Ph)$ (Ia) and $Ti(OAr\text{-}2,6\text{-}Ph_2)_2(CH_2SiMe_3)(\eta^2\text{-}PhNCCH_2SiMe_3)$ (Ib). The mono-iminoacyl complexes I are stoichiometrically related to the most widely studied η^2-acyl and η^2-iminoacyl derivatives of the group 4 metals, namely those of formula $Cp_2M(R)(\eta^2\text{-}RCX)$ (M = Ti, Zr, Hf; X = O, NR').[5,9] Actinide compounds have also been extensively studied of the type $Cp^*_2M(R)(\eta^2\text{-}RCO)$ (M = Th, U).[10] These 18-electron "metallocene" derivatives have been found to adopt two possible ground-state structures (A and B of Chart I). In both structures η^2-RCX and R lie in a plane bisecting the metallocene unit. The difference arises as to whether the heteroatom lies toward (A) or away from (B) the noninserted alkyl group. Although for the group 4 metal acyl derivatives a ground-state structure with the oxygen atom in, or proximal to, the M–R group was found,[5] Erker demonstrated that in fact the other, distal, isomer was the initial, kinetic product of the migratory insertion reaction.[4b] In the case of the thorium acyls $Cp^*_2Th(R)(\eta^2\text{-}RCO)$ both of these isomers have been structurally observed depending on the alkyl substituents.[10] However, for the related η^2-iminoacyls, $Cp_2Zr(R)(\eta^2\text{-}RCNR')$, Lappert has observed both isomers A and B present in solution by NMR studies with facile exchange taking place at elevated temperatures.[16c] Exchange between isomers of this type presumably takes place either by rotation of the η^2-RCX group or via an η^2-η^1-η^2 rearrangement involving essentially complete dissociation of the nitrogen donor atom from the metal.

The aryl oxide derivatives I do not suffer from the same electronic restrictions as these 18-electron metallocene compounds. Hence not only isomers A and B are viable ground-state structures but also geometry C has to be considered as well as all of the possible conformers in between these idealized situations. The molecular structures of Ia and Ib are shown in Figures 3 and 4, respectively, while Tables II and III contain the fractional coordinates and isotropic thermal parameters. Some pertinent bond distances and angles for the two structures are collected in Table IV. Although the coordination number is five, the structures are best described as pseudotetrahedral about the titanium atom with the η^2-iminoacyl group occupying a single coordination site. It can be seen that the ground-state conformation of the η^2-iminoacyl

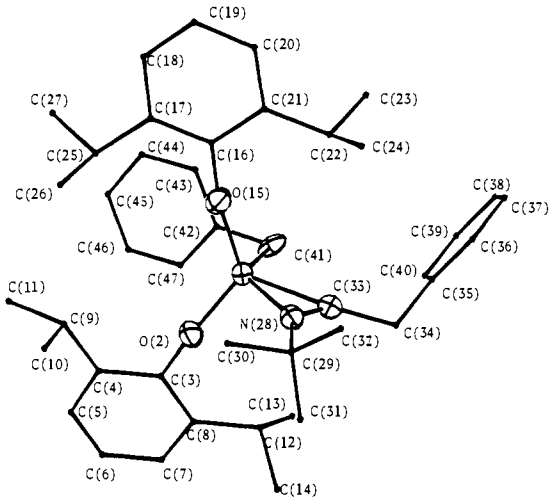

Figure 3. ORTEP view of $Ti(OAr\text{-}2,6\text{-}i\text{-}Pr_2)_2(\eta^2\text{-}t\text{-}BuNCCH_2Ph)(CH_2Ph)$ (Ia).

Table II. Fractional Coordinates and Isotropic Thermal Parameters for Ia

atom	10^4x	10^4y	10^4z	$10B_{iso}$
Ti(1)	2692.5 (5)	2074 (1)	4640 (1)	22
O(2)	1792 (2)	1684 (3)	4121 (4)	28
C(3)	1216 (3)	1568 (4)	3462 (6)	29
C(4)	551 (3)	2053 (5)	4370 (7)	38
C(5)	−15 (3)	1974 (6)	3652 (7)	47
C(6)	70 (3)	1436 (6)	2140 (8)	52
C(7)	724 (3)	948 (5)	1290 (7)	43
C(8)	1313 (3)	991 (5)	1925 (6)	30
C(9)	454 (3)	2557 (6)	6036 (7)	44
C(10)	141 (4)	1520 (6)	6675 (8)	62
C(11)	−44 (3)	3621 (6)	6772 (7)	53
C(12)	2023 (3)	440 (5)	977 (6)	35
C(13)	2458 (4)	1105 (7)	−107 (7)	55
C(14)	1858 (4)	−941 (6)	151 (9)	61
O(15)	2830 (2)	2928 (3)	6512 (4)	29
C(16)	3069 (3)	3541 (4)	7810 (5)	26
C(17)	2554 (3)	4194 (5)	9057 (6)	30
C(18)	2802 (3)	4760 (5)	10385 (6)	36
C(19)	3507 (3)	4690 (5)	10481 (6)	37
C(20)	4010 (3)	4078 (5)	9239 (6)	34
C(21)	3801 (3)	3502 (4)	7870 (6)	28
C(22)	1775 (3)	4266 (5)	8985 (7)	42
C(23)	1531 (4)	5565 (6)	9824 (7)	53
C(24)	1230 (4)	3319 (8)	9538 (10)	70
C(25)	4366 (3)	2879 (5)	6499 (6)	33
C(26)	4574 (6)	1775 (9)	6650 (10)	103
C(27)	5006 (5)	3757 (8)	6158 (10)	118
N(28)	2957 (2)	360 (4)	4143 (4)	24
C(29)	2739 (3)	−845 (5)	4403 (6)	34
C(30)	2120 (5)	−669 (6)	5701 (9)	78
C(31)	2477 (9)	−1758 (8)	3131 (10)	144
C(32)	3355 (6)	−1231 (15)	4670 (23)	201
C(33)	3445 (3)	796 (4)	3256 (5)	26
C(34)	4059 (3)	210 (5)	2004 (6)	40
C(35)	4741 (3)	1113 (5)	1747 (5)	29
C(36)	5373 (3)	1154 (5)	2244 (6)	37
C(37)	6001 (3)	1998 (6)	2028 (6)	42
C(38)	5996 (3)	2808 (5)	1332 (6)	39
C(39)	5373 (3)	2776 (5)	833 (6)	36
C(40)	4750 (3)	1939 (5)	1048 (6)	31
C(41)	3214 (3)	3415 (5)	3570 (6)	30
C(42)	2709 (3)	4384 (5)	4326 (6)	29
C(43)	2802 (3)	5331 (5)	5653 (6)	35
C(44)	2287 (4)	6169 (5)	6421 (7)	43
C(45)	1665 (4)	6096 (5)	5905 (7)	47
C(46)	1567 (3)	5179 (6)	4575 (8)	43
C(47)	2078 (3)	4351 (5)	3811 (6)	34

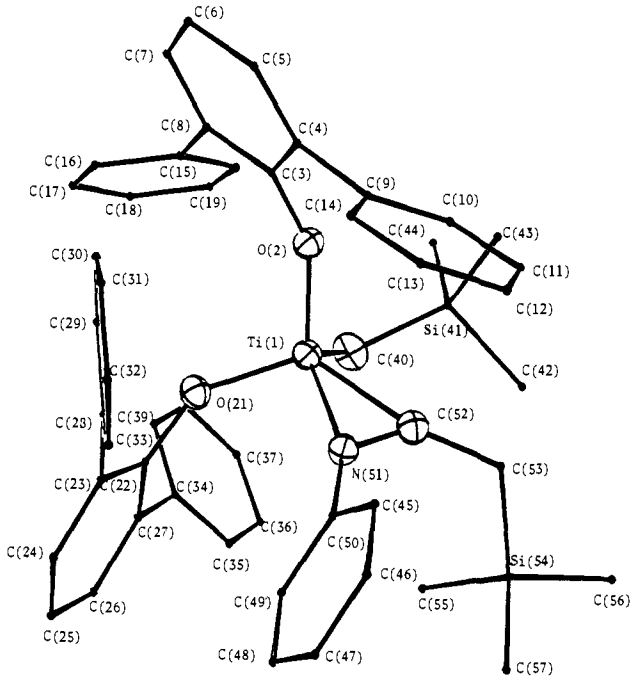

Figure 4. ORTEP view of $Ti(OAr\text{-}2,6\text{-}Ph_2)_2(\eta^2\text{-}PhNCCH_2SiMe_3)(CH_2SiMe_3)$ (Ib).

is such that the CN vector points toward the noninserted Ti–R function, structure B (Chart I). In compound Ia the C–N and Ti–C(R) vectors are essentially coplanar, while in Ib there is a slight (10°) rotation of the CN unit toward geometry C. The ^1H and ^{13}C NMR spectra of the mono-insertion compounds I shows only one set of peaks even at low temperature. Furthermore, the methylene protons of the CH_2Ph and CH_2SiMe_3 groups remain as sharp singlets (Figure 1). These data are consistent with the observed solid-state structure being maintained in solution, although highly fluxional structures of lower symmetry such as C cannot be entirely ruled out. Further structural information is provided by the ^1H NMR of Ia. At all temperatures studied (up to 50 °C) only one type of methyne proton ($CHMe_2$) of the isopropyl group of the OAr-2,6-*i*-Pr_2 ligand was observed, indicating that rapid rotation about the Ti–O–Ar bonds is occurring. However, the isopropyl-methyl groups ($CHMe_2$) were found to be diastereotopic, yielding two well resolved doublets (Figure 1). In the ^{13}C NMR two distinct $CHMe_2$ carbon resonances were also observed. These data are as one would expect for the observed structure, or in general for any tetrahedral $(ArO\text{-}2,6\text{-}i\text{-}Pr_2)_2M(X)(Y)$ compound, given the lack of a plane of symmetry through the *i*-Pr_2 groups. Furthermore, the lack of rapid equilibration of the isopropyl *i*-Pr methyl groups mean that "inversion" at the pseudotetrahedral titanium metal center (presumably via a pseudo-square-planar geometry) does not occur.

$Zr(OAr\text{-}2,6\text{-}t\text{-}Bu_2)_2(\eta^2\text{-}t\text{-}BuNCCH_2Ph)_2$ (IId) and $Hf(OAr\text{-}2,6\text{-}t\text{-}Bu_2)_2(\eta^2\text{-}PhNCCH_3)_2$ (IIg). Compounds IId and IIg represent the first molecules to be structurally characterized containing two η^2-iminoacyl groups. Although the carbonylation of the metallocene dialkyls Cp_2MR_2 and $Cp^*_2MR_2$ to produce the corresponding ene-diolates has been proposed to proceed via a bis-acyl complex, detection of this potentially 20-electron intermediate has not been reported.[24] However, Marks et al. have isolated and structurally characterized a bis-η^2-carbamoyl formed by insertion of 2 equiv of CO in the M–N bonds of $Cp^*_2M(NMe_2)_2$ (M = Th, U).[21] The solid-state structure shows the two η^2-carbamoyl ligands in $Cp^*_2U(\eta^2\text{-}Me_2NCO)_2$ to be close to coplanar with the carbon atoms cis to each other, although the complexes do not undergo further reaction on thermolysis.

The molecular structures of Id and IIg are shown in Figure 5 and 6 along with the numbering scheme used. Tables V and VI contain the fractional coordinates and isotropic thermal parameters, while Table VII contains some pertinent bond distances and angles. We envisage a total of five possible idealized ground-state

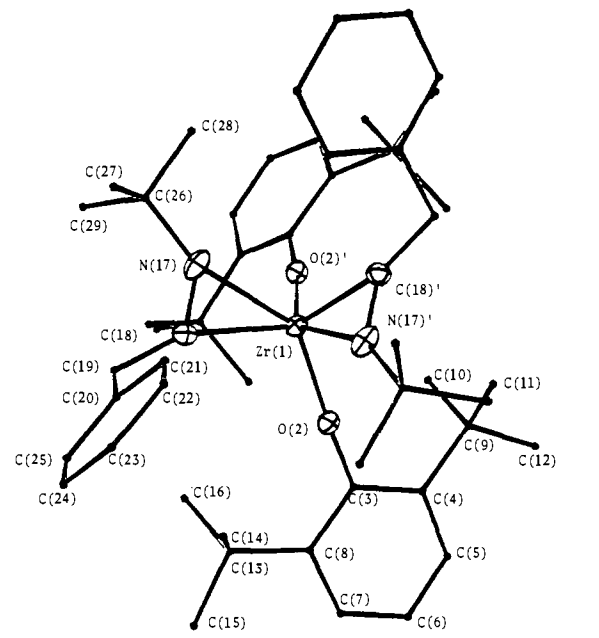

Figure 5. ORTEP view of $Zr(OAr\text{-}2,6\text{-}t\text{-}Bu_2)_2(\eta^2\text{-}t\text{-}BuNCCH_2Ph)_2$ (IId).

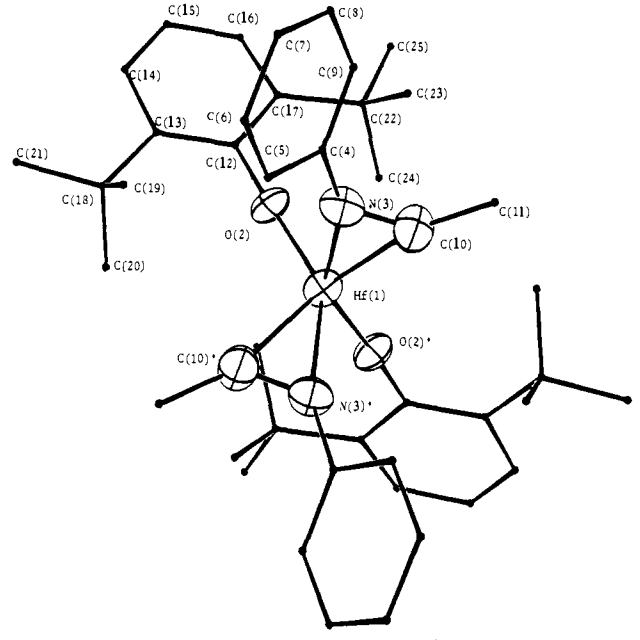

Figure 6. ORTEP view of $Hf(OAr\text{-}2,6\text{-}t\text{-}Bu_2)_2(\eta^2\text{-}PhNCMe)_2$ (IIg).

Chart II

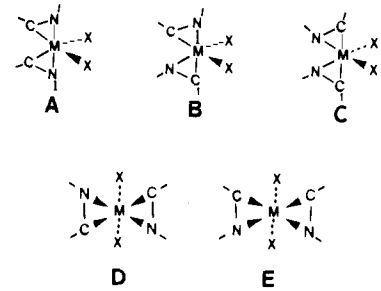

structures for molecules of the type $X_2M(\eta^2\text{-}RNCR')_2$ (Chart II), the uranium complex mentioned earlier falling into category A. However, it can be seen that the structures of IId and IIg are significantly different and are more consistent with conformer D. Although formally six coordinate the molecules are again best described as pseudotetrahedral about the metal atom with the η^2-iminoacyl units occupying a single site. The two iminoacyl CN

Table III. Fractional Coordinates and Isotropic Thermal Parameters for Ib

atom	10^4x	10^4y	10^4z	$10B_{iso}$
Ti(1)	2588.7 (5)	3232 (1)	5700 (1)	18
O(2)	3077 (2)	1789 (3)	6343 (4)	20
C(3)	3589 (3)	924 (5)	6485 (6)	20
C(4)	4069 (2)	855 (5)	7734 (6)	20
C(5)	4597 (3)	−26 (5)	7827 (6)	25
C(6)	4654 (3)	−831 (6)	6720 (7)	27
C(7)	4185 (3)	−752 (6)	5510 (6)	26
C(8)	3649 (3)	117 (5)	5350 (6)	23
C(9)	4039 (2)	1745 (5)	8934 (6)	20
C(10)	3530 (3)	2022 (6)	9431 (6)	25
C(11)	3530 (3)	2800 (6)	10610 (6)	29
C(12)	4045 (3)	3328 (5)	11280 (7)	28
C(13)	4545 (3)	3057 (6)	10773 (6)	26
C(14)	4546 (3)	2283 (5)	9623 (6)	24
C(15)	3157 (3)	165 (5)	3985 (6)	26
C(16)	3323 (3)	200 (6)	2775 (7)	32
C(17)	2879 (4)	186 (6)	1491 (7)	39
C(18)	2286 (4)	146 (6)	1406 (8)	40
C(19)	2117 (3)	102 (6)	2596 (7)	37
C(20)	2553 (3)	115 (6)	3875 (7)	28
O(21)	2770 (2)	3661 (3)	4169 (4)	21
C(22)	2852 (3)	4654 (5)	3629 (6)	20
C(23)	3431 (3)	5031 (5)	4053 (6)	22
C(24)	3478 (3)	6110 (6)	3541 (6)	26
C(25)	2978 (3)	6823 (6)	2645 (7)	30
C(26)	2419 (3)	6401 (6)	2211 (7)	28
C(27)	2350 (3)	5307 (5)	2672 (6)	23
C(28)	3978 (2)	4309 (5)	5024 (5)	18
C(29)	4400 (3)	4899 (6)	6046 (7)	25
C(30)	4920 (3)	4225 (6)	6900 (7)	28
C(31)	5039 (3)	2950 (6)	6772 (6)	25
C(32)	4623 (3)	2367 (5)	5767 (6)	23
C(33)	4101 (3)	3029 (5)	4905 (6)	21
C(34)	1764 (3)	4834 (5)	2138 (5)	23
C(35)	1746 (3)	3671 (6)	1501 (6)	27
C(36)	1202 (3)	3215 (6)	970 (7)	31
C(37)	659 (3)	3926 (6)	1110 (7)	34
C(38)	660 (3)	5075 (6)	1743 (7)	33
C(39)	1207 (3)	5529 (6)	2246 (6)	29
C(40)	1690 (3)	2886 (6)	4850 (6)	24
Si(41)	11300 (1)	2168 (2)	5833 (2)	29
C(42)	695 (4)	3360 (7)	6346 (9)	48
C(43)	1831 (3)	1439 (6)	7433 (8)	41
C(44)	906 (4)	929 (8)	4751 (9)	54
C(45)	2995 (3)	6771 (5)	6578 (6)	24
C(46)	3288 (3)	7759 (6)	7124 (8)	34
C(47)	3673 (3)	7772 (7)	8451 (8)	40
C(48)	3771 (3)	6796 (7)	9259 (7)	40
C(49)	3485 (3)	5790 (6)	8732 (7)	32
C(50)	3094 (3)	5787 (5)	7410 (6)	23
N(51)	2779 (2)	4771 (4)	6880 (4)	19
C(52)	2370 (2)	4414 (5)	7290 (6)	21
C(53)	2083 (3)	5015 (5)	8353 (6)	24
Si(54)	1500 (1)	6486 (2)	7778 (2)	26
C(55)	1865 (3)	7875 (6)	8483 (7)	34
C(56)	844 (3)	6518 (6)	8497 (8)	39
C(57)	1220 (3)	6503 (6)	5881 (7)	36
C(58)	274 (5)	473 (9)	−1524 (11)	76
C(59)	335 (5)	120 (9)	62 (12)	81
C(60)	−246 (6)	1415 (10)	−2098 (14)	110

vectors are oriented parallel with each other (crystallographic C_2 axis) in a head-to-tail fashion. Although the idealized geometry D would require these vectors to be parallel with the OMO (M = Zr, Hf) plane, they are in fact tilted from it by 21.5° and 34.5°, respectively. This twisting of the CN vectors to give the observed ground-state structure has been predicted on the basis of theoretical studies by Tatsumi et al.[25] and hence is not a consequence of steric pressure. The O–M–O angles of 97.3 (1)° in IId and 103.6 (2)° in IIg are smaller than the angle of 116.2 (2)° found in the complex Zr(OAr-2,6-*t*-Bu)(OAr-2,6-*t*-Bu-40Me)(CH_2Ph)$_2$ and those found in Ia and Ib, 124.4 (2) and 110.4 (2)°, respectively.

(25) Tatsumi, K., personal communication.

Table IV. Selected Bond Distance (Å) and Angles (deg) for Ia and Ib

Ia		Ib	
Ti–O(2)	1.811 (3)	Ti–O(2)	1.821 (4)
Ti–O(15)	1.816 (3)	Ti–O(21)	1.850 (4)
Ti–N(28)	2.015 (4)	Ti–N(51)	2.025 (5)
Ti–C(33)	2.096 (5)	Ti–C(52)	2.086 (6)
Ti–C(41)	2.147 (5)	Ti–C(40)	2.092 (6)
C(33)–N(28)	1.257 (6)	C(52)–N(51)	1.279 (7)
C(29)–N(28)	1.486 (6)	C(50)–N(51)	1.435 (7)
O(2)–Ti–O(15)	124.4 (2)	O(21)–Ti–O(2)	110.4 (2)
O(2)–Ti–N(28)	99.9 (2)	O(21)–Ti–N(51)	96.1 (2)
O(2)–Ti–C(33)	112.5 (2)	O(21)–Ti–C(52)	127.0 (2)
O(2)–Ti–C(41)	100.2 (2)	O(21)–Ti–C(40)	102.3 (2)
O(15)–Ti–N(28)	105.9 (2)	O(2)–Ti–N(51)	116.2 (2)
O(15)–Ti–C(33)	117.2 (2)	O(2)–Ti–C(52)	112.2 (2)
O(15)–Ti–C(41)	100.7 (2)	O(2)–Ti–C(40)	107.2 (2)
N(28)–Ti–C(33)	35.5 (2)	N(51)–Ti–C(52)	36.2 (2)
N(28)–Ti–C(41)	128.4 (2)	N(51)–Ti–C(40)	122.6 (2)
C(33)–Ti–C(41)	92.9 (2)	C(40)–Ti–C(52)	93.9 (2)
Ti–O(2)–C(3)	163.8 (3)	Ti–O(2)–C(3)	152.7 (3)
Ti–O(15)–C(16)	169.5 (3)	Ti–O(21)–C(22)	40.3 (3)
Ti–C(33)–N(28)	68.7 (3)	Ti–C(52)–N(51)	69.3 (3)
Ti–N(28)–C(33)	75.8 (3)	Ti–N(51)–C(52)	74.5 (3)

Table V. Fractional Coordinates and Isotropic Thermal Parameters for IId

atom	10^4x	10^4y	10^4z	$10B_{iso}$
Zr(1)	0*	−2053.7 (4)	2500*	12
O(2)	−756 (1)	−858 (2)	2185 (1)	14
C(3)	−1314 (1)	−157 (3)	1903 (2)	14
C(4)	−1519 (1)	578 (3)	1261 (2)	14
Cke	−2118 (2)	1239 (3)	956 (2)	19
C(6)	−2500 (2)	1211 (3)	1263 (2)	24
C(7)	−2283 (2)	544 (3)	1899 (2)	21
C(8)	−1692 (1)	−138 (3)	2246 (2)	16
C(9)	−1096 (1)	743 (3)	911 (2)	15
C(10)	9602 (2)	1267 (3)	1501 (2)	17
C(11)	−1037 (2)	−420 (3)	578 (2)	17
C(12)	8571 (2)	1637 (3)	249 (2)	18
C(13)	8515 (2)	9177 (3)	2975 (2)	18
C(14)	−1564 (2)	−2164 (3)	2827 (2)	20
C(15)	8060 (2)	9523 (3)	3263 (2)	22
C(16)	−756 (2)	−526 (3)	3626 (2)	21
N(17)	687 (1)	−3298 (2)	3429 (1)	16
C(18)	143 (1)	−3219 (3)	3428 (2)	15
C(19)	−6 (2)	−3761 (3)	3968 (2))	20
C(20)	−479 (2)	−4828 (3)	3657 (2)	19
C(21)	−533 (2)	−5562 (3)	3099 (2)	23
C(22)	9061 (2)	3432 (3)	2857 (2)	26
C(23)	8695 (2)	3140 (3)	3161 (2)	28
C(24)	8738 (2)	3866 (4)	3710 (2)	33
C(25)	−856 (2)	−5129 (3)	3960 (2)	26
C(26)	1351 (2)	−3942 (3)	3973 (2)	20
C(27)	1225 (2)	−5264 (3)	4022 (2)	26
C(28)	1792 (2)	−3805 (3)	3665 (2)	24
C(29)	1698 (2)	6649 (4)	4746 (2)	26

The benzyl derivatives IIa–d should allow one to differentiate structures A–C from D and E (Chart II) in solution as the latter two do not possess a plane of symmetry passing through the methylene carbon of the R′NCCH_2Ph group. Hence in a static structure an AB or AX pattern should be observed. However, all of the complexes II exhibit only one sharp set of ^{1}H NMR resonances at ambient temperatures and furthermore the benzyl groups of IIa–d appear as sharp singlets. On cooling toluene-d_8 solutions of the benzyl derivatives, some broadening of both the R′NCCH_2Ph and aryl oxide resonances is seen. This temperature change is most dramatic for complexes formed by insertion of the bulky 2,6-dimethylphenyl isocyanide, IIb and IIc. In the case of IIc the benzyl protons do not resolve out completely at −70 °C (200 MHz) although two nonequivalent *t*-Bu groups of the aryl oxide ligand are well resolved. These changes in the ^{1}H NMR spectra we ascribe to the slowing down of the process depicted (Scheme IV) in which the η^2-iminoacyl groups undergo a flipping

Table VI. Fractional Coordinates and Isotropic Thermal Parameters for IIg

atom	10^4x	10^4y	10^4z	$10B_{iso}$
Hf	0	14361 (2)	$^1/_4$	3.196 (6)
O	0474 (3)	2243 (3)	1894 (2)	3.46 (8)
N	-0434 (4)	0394 (3)	1756 (2)	3.6 (1)
C(1)	-0329 (3)	-0244 (4)	1283 (3)	4.0 (1)
C(2)	0374 (6)	-0911 (5)	1462 (4)	5.4 (2)
C(3)	0504 (7)	-1543 (5)	1018 (5)	7.3 (2)
C(4)	-0081 (6)	-1496 (6)	0398 (4)	7.6 (2)
C(5)	-0754 (7)	-0834 (8)	0224 (4)	8.0 (3)
C(6)	-0907 (6)	-0193 (6)	0652 (3)	6.0 (2)
C(7)	-1261 (5)	0606 (4)	1933 (3)	4.2 (1)
C(8)	-2305 (6)	0218 (6)	1681 (4)	6.6 (2)
C(101)	0784 (5)	2683 (4)	1415 (3)	3.7 (1)
C(102)	1808 (5)	2563 (4)	1326 (3)	4.1 (1)
C(103)	2087 (6)	3017 (5)	0814 (3)	5.3 (2)
C(104)	1411 (7)	3581 (5)	0425 (3)	6.0 (2)
C(105)	0437 (7)	3709 (4)	0523 (3)	5.2 (2)
C(106)	0079 (6)	3265 (4)	1006 (3)	4.4 (1)
C(120)	2611 (5)	1961 (5)	1752 (3)	4.8 (2)
C(121)	2252 (6)	1004 (5)	1673 (4)	5.1 (2)
C(122)	2819 (5)	2255 (5)	2456 (4)	5.4 (2)
C(123)	3672 (7)	1984 (7)	1575 (5)	7.6 (2)
C(160)	-1062 (6)	3397 (4)	1063 (3)	5.0 (2)
C(161)	-1655 (6)	2528 (5)	0937 (4)	5.5 (2)
C(162)	-1091 (7)	3761 (5)	1734 (4)	5.9 (2)
C(163)	-1651 (7)	4060 (6)	0578 (4)	7.1 (2)

Table VII. Selected Bond Distances (Å) and Angles (deg) for IId and IIg

IId		IIg	
Zr-O(2)	2.027 (2)	Hf-O	1.978 (4)
Zr-N(17)	2.221 (3)	Hf-N	2.212 (5)
Zr-C(18)	2.228 (3)	Hf-C(7)	2.209 (6)
N(17)-C(18)	1.286 (4)	N-C(7)	1.275 (8)
N(17)-C(26)	1.428 (4)	N-C(1)	1.422 (8)
O(2)-Zr-O(2)′	97.3 (1)	O-Hf-O′	103.6 (2)
O(2)-Zr-N(17)	92.5 (1)	O-Hf-N	92.6 (2)
O(2)-Zr-C(18)	114.8 (1)	O-Hf-C(7)	113.2 (2)
N(17)-Zr-N(17)′	102.3 (1)	N-Hf-N′	89.0 (3)
C(18)-Zr-C(18)′	108.3 (2)	C(7)-Hf-C(7)′	110.6 (4)
N(17)-Zr-C(18)	33.6 (1)	N-Hf-C(7)	33.5 (2)
Zr-O(2)-C(3)	172.7 (2)	Hf-O-C(101)	170.8 (4)
Zr-C(18)-N(17)	72.9 (2)	Hf-C(7)-N	73.4 (4)
Zr-N(17)-C(18)	73.5 (2)	Hf-N-C(7)	73.1 (4)

Scheme IV

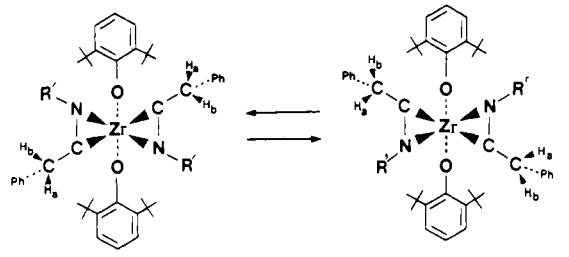

of their head-to-tail arrangement. The effect is to interchange the two enantiomers shown and to also equilibrate the diastereotopic benzyl protons on the ^{1}H NMR time scale. The slowing down of this process also results in the aryl oxide *t*-Bu groups becoming nonequivalent, as is the case in the structure of IId and IIg. This implies that rotation about the M–O–Ar bonds is restricted in these very crowded molecules and is occurring at a rate less than or equal to η^2-iminoacyl flipping. An activation energy $\Delta G^{\ddagger}$ at coalescence temperature (T_c) was estimated as 10.3 ± 0.5 (−65 °C) for IIb and 11.4 ± 0.5 (−40 °C) for IIc for this process.

The exchange of the two enantiomers by iminoacyl flipping could occur by rotation of the η^2-iminoacyl MCN plane with little change in M–N bonding, or it could also involve an η^2-η^1 (rotation)-η^2 transformation. Slow exchange on the NMR time scale

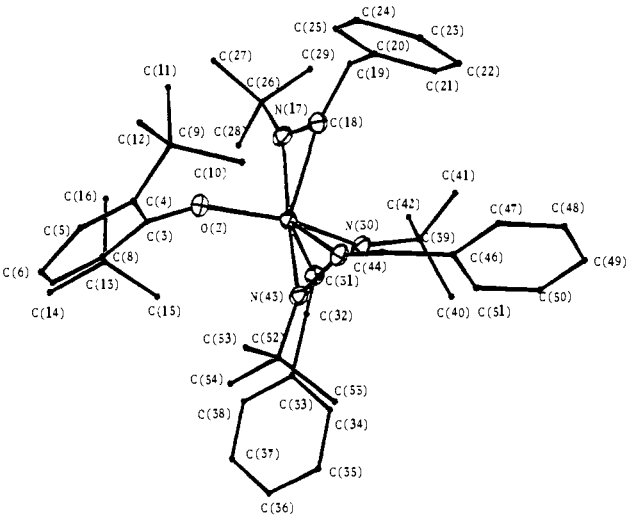

Figure 7. ORTEP view of Zr(OAr-2,6-*t*-Bu$_2$)(η^2-*t*-BuNCCH$_2$Ph)$_3$ (IVa).

Scheme V

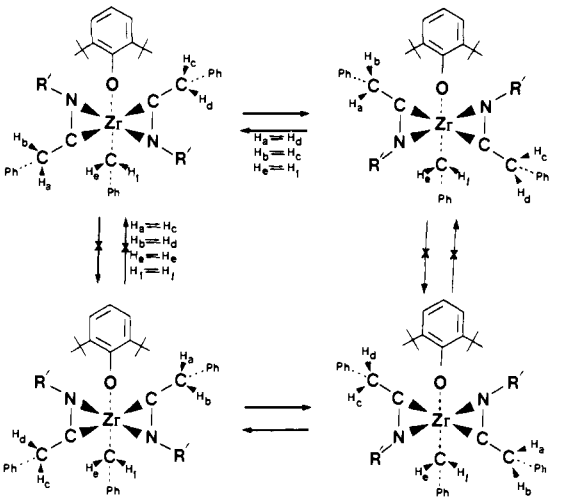

between the two isomers of Cp$_2$Zr(η^2-*p*-tolNCCH(SiMe$_3$)$_2$)(Cl) was observed by Lappert et al.;[16d] again the exchange involves the formal rotation of an η^2-iminoacyl group by either of these two pathways. Given the molecules and techniques available it is difficult to see any way that these two pathways could be differentiated. Hoffman et al. have carried out extensive theoretical studies on the acyl complexes Cp$_2$Zr(COCH$_3$)(CH$_3$) using the EHMO method.[11] They found that the isomerization process from η^2-O-outside to η^2-O-inside proceeded through an η^2-η^1-(rotation)-η^2 motion. However, the M(OAr)$_2$ (M = Ti, Zr, Hf) fragments possess less electronic restrictions than the corresponding M(Cp)$_2$ units and hence a direct η^2-rotation may be available.

The bis-inserted complex III is related to the molecules II in that it contains two η^2-iminoacyl groups and two monodentate ligands. The room temperature ^{1}H NMR spectrum of III shows the benzyl protons of the η^2-xyNCCH$_2$Ph group as an AB pattern with a singlet for the noninserted Zr-*CH*$_2$Ph protons. This observation is consistent with III adopting an analogous structure to II with the noninserted benzyl replacing one of the aryl oxide ligands (Scheme V). Even with the facile rotation of the η^2-iminoacyl groups that takes place, it is impossible to exchange these diastereotopic benzyl protons without adopting a square-planar coordination about the metal atom (Scheme V); cf. the discussion of molecule Ia above.

Zr(OAr-2,6-*t*-Bu$_2$)(η^2-*t*-BuNCCH$_2$Ph)$_3$ (IVa). The molecular structure of IVa is shown in Figure 7 along with the numbering scheme used. Table VIII contains the fractional coordinates while some important bond distances and angles are given in Table IX. It can be seen that all three of the iminoacyl groups are η^2-bound, giving a formally seven coordinate zirconium complex. However,

Table VIII. Fractional Coordinates and Isotropic Thermal Parameters for IVa

atom	10^4x	10^4y	10^4z	$10B_{iso}$
Zr(1)	2476.4 (2)	7855.9 (2)	1913.3 (3)	13
O(2)	2965 (2)	7201 (1)	192 (2)	15
C(3)	3216 (2)	6467 (2)	-685 (3)	13
C(4)	2516 (2)	5902 (2)	-1748 (3)	15
C(5)	2762 (3)	5074 (2)	-2500 (3)	20
C(6)	3667 (3)	4813 (2)	-2272 (4)	23
C(7)	4377 (3)	5420 (2)	-1353 (3)	19
C(8)	4187 (2)	6261 (2)	-576 (3)	16
C(9)	1546 (3)	6204 (2)	-2174 (3)	19
C(10)	1751 (3)	7103 (3)	-2407 (4)	23
C(11)	990 (3)	5526 (3)	-3461 (4)	25
C(12)	854 (2)	6312 (2)	-1158 (4)	20
C(13)	5044 (2)	6973 (2)	258 (3)	19
C(14)	6023 (3)	6621 (3)	44 (4)	26
C(15)	5016 (3)	7795 (3)	-199 (4)	26
C(16)	5025 (3)	7251 (3)	1734 (4)	24
N(17)	2017 (2)	6550 (2)	2137 (3)	13
C(18)	1241 (2)	6913 (2)	2029 (3)	14
C(19)	201 (3)	6508 (2)	1881 (4)	20
C(20)	-346 (2)	6957 (2)	2974 (3)	17
C(21)	104 (3)	7346 (3)	4262 (4)	27
C(22)	-419 (3)	7741 (3)	5259 (4)	34
C(23)	-1409 (3)	7741 (3)	4976 (4)	31
C(24)	1864 (3)	7351 (3)	3703 (4)	30
C(25)	-1336 (3)	6968 (2)	2714 (4)	23
C(26)	2197 (3)	5640 (2)	2196 (3)	17
C(27)	3290 (3)	5628 (2)	2361 (4)	21
C(28)	1810 (3)	5504 (3)	3374 (4)	24
C(29)	1733 (3)	4903 (2)	910 (4)	21
N(30)	2602 (2)	8744 (2)	4028 (3)	16
C(31)	3406 (2)	8412 (2)	3894 (3)	16
C(32)	4313 (3)	8609 (2)	4890 (3)	20
C(33)	4609 (2)	7798 (2)	5225 (3)	18
C(34)	3980 (3)	7323 (3)	5729 (4)	22
C(35)	4252 (3)	6596 (3)	6082 (4)	27
C(36)	5161 (3)	6337 (3)	5941 (4)	29
C(37)	5802 (3)	6808 (3)	5446 (4)	28
C(38)	5519 (3)	7528 (3)	5092 (4)	22
C(39)	2299 (3)	9454 (2)	5160 (3)	21
C(40)	2273 (3)	9122 (3)	6326 (4)	26
C(41)	2990 (3)	10327 (3)	5544 (4)	29
C(42)	1295 (3)	9626 (3)	4674 (4)	27
N(43)	2701 (2)	9149 (2)	1481 (3)	17
C(44)	1788 (2)	8940 (2)	1333 (3)	17
C(45)	1001 (3)	9453 (3)	936 (4)	24
C(46)	32 (3)	8883 (3)	435 (4)	23
C(47)	-200 (3)	8365 (3)	-871 (4)	31
C(48)	-1071 (3)	7813 (3)	-1352 (5)	36
C(49)	-1512 (3)	8307 (4)	779 (5)	47
C(50)	-1730 (3)	7785 (3)	-520 (5)	37
C(51)	-636 (3)	8847 (3)	1254 (4)	38
C(52)	3300 (3)	9920 (2)	1327 (3)	20
C(53)	4313 (3)	9943 (3)	2031 (4)	24
C(54)	3302 (3)	9734 (3)	-130 (4)	27
C(55)	2919 (3)	10814 (3)	1961 (4)	30

Table IX. Selected Bond Distances (Å) and Angles (deg) for IVa

Zr-O(2)	2.058 (2)	N(17)-C(18)	1.277 (4)
Zr-N(17)	2.211 (3)	N(17)-C(26)	1.498 (4)
Zr-N(30)	2.257 (3)	N(30)-C(31)	1.284 (4)
Zr-N(43)	2.248 (3)	N(30)-C(39)	1.506 (4)
Zr-C(18)	2.241 (3)	N(43)-C(44)	1.276 (4)
Zr-C(31)	2.249 (4)	N(43)-C(52)	1.493 (4)
Zr-C(44)	2.251 (3)		
O(2)-Zr-N(17)	90.7 (1)	N(17)-Zr-N(30)	98.5 (1)
O(2)-Zr-N(30)	156.31 (9)	N(17)-Zr-N(43)	170.5 (1)
O(2)-Zr-N(43)	88.6 (1)	N(17)-Zr-C(18)	33.3 (1)
O(2)-Zr-C(18)	105.3 (1)	N(17)-Zr-C(31)	94.3 (1)
O(2)-Zr-C(31)	124.9 (1)	N(17)-Zr-C(44)	138.1 (1)
O(2)-Zr-C(44)	99.2 (1)	N(30)-Zr-N(43)	85.7 (1)
C(18)-Zr-C(31)	108.4 (1)	N(30)-Zr-C(18)	94.1 (1)
C(18)-Zr-C(44)	105.4 (1)	N(30)-Zr-C(31)	33.1 (1)
C(31)-Zr-C(44)	111.9 (1)	N(30)-Zr-C(44)	88.4 (1)
N(43)-Zr-C(18)	138.2 (1)	Zr-N(43)-C(44)	73.7 (2)
N(43)-Zr-C(31)	93.9 (1)	Zr-C(15)-N(17)	72.0 (2)
N(43)-Zr-C(44)	32.9 (1)	Zr-C(31)-N(30)	73.8 (2)
Zr-O(2)-C(3)	152.8 (2)	Zr-C(44)-N(43)	73.4 (2)
Zr-N(17)-C(18)	74.6 (2)		
Zr-N(30)-C(31)	73.1 (2)		

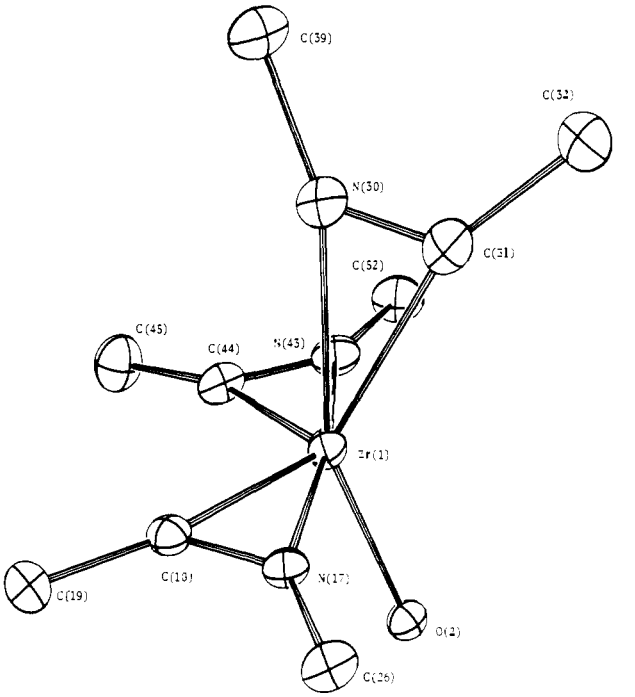

Figure 8. ORTEP view of $Zr(OAr\text{-}2,6\text{-}t\text{-}Bu_2)(\eta^2\text{-}t\text{-}BuNCCH_2Ph)_3$ (IVa) emphasizing the central metal environment.

the structure can also be considered as pseudo-tetrahedral with each of the η^2-iminoacyl units occupying a single coordination site. The structure can be simplified by using the views shown, Figure 8, containing in the idealized situation two types of η^2-iminoacyl groups in the ratio of 2:1. The unique η^2-iminoacyl lies in a plane containing the Zr–O bond, with the C–N vector pointing away. The other two iminoacyls then are arranged co-planar with each other, with carbon atoms cis (Figure 8). The Zr–O–N(30)C(31) plane is almost exactly perpendicular to the ZrN(17)C(18)N(43)C(44) plane. The orientation of the two equivalent η^2-iminoacyl groups is one that one might expect to be the intermediate situation leading to their intramolecular coupling although the C(18)–C(44) distance is nonbonding. However, theoretical studies have indicated that the least motion pathway leading from this situation to an ene-diamide ligand is symmetry disallowed.[24,25]

Spectroscopically one would predict two types of iminoacyl group in the ^1H and ^{13}C NMR spectrum based on the observed solid-state structure. At 25 °C only one set of resonances is observed for both IVa and IVb. However, on cooling solutions of IVb in toluene-d_8, the η^2-xyNCCH_2Ph protons which are initially a singlet split out into an AB pattern and a new singlet of total intensity ratio of 2:1. The AB pattern is due to the two coplanar η^2-iminoacyl groups that do not reside on a mirror plane while the singlet is assigned to the third, unique η^2-iminoacyl that lies on a virtual plane of symmetry (Figure 8). The activation energy for exchange of these nonequivalent groups can be estimated from the coalescence temperature as $\Delta G^{\ddagger}(T_c) = 13.0 \pm 0.5$ (+2 °C). In complex IVa the benzyl protons remain as a single sharp singlet down to −65 °C, indicating that the exchange process is faster for less bulky *t*-BuNC derivatives. The low-temperature ^{13}C NMR spectrum of IVb also shows two nonequivalent xyNCCH_2Ph carbon resonances at δ 247.1 and 262.3. On warming, these signals broaden and collapse into the base line at ambient temperatures. However, IVa only exhibits one sharp signal for these carbon atoms, consistent with the ^1H NMR results above. Again two limiting processes for exchange of nonequivalent η^2-iminoacyl groups is possible: simple rotation or an η^2-η^1(rotation)-η^2 pathway.

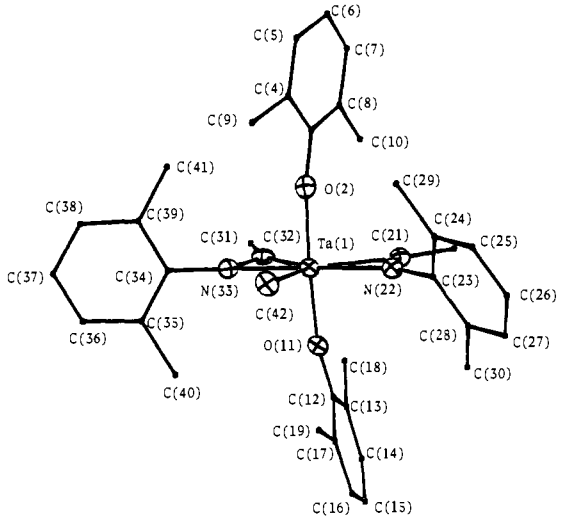

Figure 9. ORTEP view of $Ta(OAr\text{-}2,6\text{-}Me_2)_2(\eta^2\text{-}xyNCMe)_2(Me)$ (VIa).

Table X. Fractional Coordinates and Isotropic Thermal Parameters for VIa

atom	10^4x	10^4y	10^4z	$10B_{iso}$
Ta(1)	-25.6 (3)	2475.0 (2)	3812.3 (3)	14
O(2)	1731 (4)	1875 (2)	4009 (5)	17
C(3)	3042 (6)	1582 (4)	4162 (8)	19
C(4)	3827 (6)	1177 (4)	5459 (8)	23
C(5)	5171 (8)	891 (5)	5637 (10)	34
C(6)	5727 (7)	981 (5)	4513 (10)	32
C(7)	4926 (7)	1362 (4)	3228 (9)	27
C(8)	3572 (7)	1674 (4)	3031 (7)	20
C(9)	3202 (8)	1080 (5)	6651 (9)	35
C(10)	2712 (9)	2115 (5)	1662 (10)	34
O(11)	-1778 (4)	3136 (2)	3498 (5)	19
C(12)	-2889 (6)	3697 (3)	3189 (7)	16
C(13)	-3030 (6)	4268 (4)	2251 (7)	17
C(14)	-4147 (7)	4862 (4)	2017 (8)	22
C(15)	-5118 (6)	4886 (4)	2704 (8)	25
C(16)	-4996 (7)	4291 (4)	3567 (8)	21
C(17)	-3899 (6)	3701 (4)	3833 (7)	19
C(18)	-2000 (8)	4259 (4)	1436 (9)	28
C(19)	-3798 (7)	3053 (5)	4739 (9)	27
C(20)	-912 (7)	2221 (4)	-355 (8)	25
C(21)	-605 (6)	2176 (4)	1321 (7)	19
N(22)	-830 (5)	1674 (3)	1983 (6)	17
C(23)	-1471 (6)	1039 (3)	1405 (7)	17
C(24)	-733 (7)	307 (4)	1728 (7)	20
C(25)	-1384 (8)	-301 (4)	1235 (9)	27
C(26)	-2705 (8)	-175 (4)	436 (9)	28
C(27)	-3427 (7)	553 (4)	123 (8)	27
C(28)	-2838 (7)	1181 (4)	588 (7)	22
C(29)	742 (7)	169 (4)	2601 (8)	24
C(30)	-3647 (7)	1970 (4)	281 (9)	29
C(31)	1316 (7)	4182 (4)	4333 (8)	26
C(32)	821 (6)	3502 (4)	4424 (8)	20
N(33)	813 (5)	3266 (3)	5669 (6)	17
C(34)	1309 (6)	3531 (3)	7251 (7)	15
C(35)	393 (7)	3827 (4)	8092 (8)	20
C(36)	873 (7)	4032 (4)	9667 (8)	20
C(37)	2214 (7)	3955 (4)	10373 (8)	22
C(38)	3130 (7)	3668 (4)	9540 (8)	21
C(39)	2694 (6)	3453 (3)	7971 (7)	18
C(40)	-1080 (7)	3902 (4)	7299 (8)	24
C(41)	3689 (7)	3151 (4)	7076 (8)	24
C(42)	-361 (7)	1831 (4)	5479 (8)	22

$Ta(OAr\text{-}2,6\text{-}Me_2)_2(\eta^2\text{-}xyNCCH_3)_2(CH_3)$ (VIa). The molecular structure of the bis-inserted complex VIa is shown in Figure 9. Table X contains the fractional coordinates and isotropic thermal parameters while Table XI contains some pertinent bond distances and angles. It can be seen that the molecule adopts a structure in which the η^2-iminoacyl groups lie in a plane containing the metal atom and unique, noninserted $Ta\text{-}CH_3$ carbon atoms. The aryl oxide oxygen atoms are then arranged perpendicular to this plane and mutually trans. The geometry about the seven coordinate tantalum atom can hence be considered as approximating to a pentagonal bipyramid, a not uncommon coordination environment for this metal. However, an alternative picture due to the small bite of the η^2-iminoacyl groups is of a trigonal bipyramidal structure with two of these units in equatorial positions. The carbon atoms of the η^2-iminoacyl groups are arranged mutually cis with a C-Ta-C angle of 111.8 (2)°. This arrangement is reminiscent of that found in $Zr(OAr\text{-}2,6\text{-}t\text{-}Bu)_2(\eta^2\text{-}t\text{-}BuNCCH_2Ph)_3$ (IVa) above, with the groups seemingly poised to undergo intramolecular carbon–carbon coupling.

Table XI. Selected Bond Distances (Å) and Angles (deg) for VIa

Ta-O(2)	1.913 (4)	Ta-C(42)	2.232 (7)
Ta-O(11)	1.938 (4)	N(22)-C(21)	1.281 (8)
Ta-N(22)	2.151 (5)	N(22)-C(23)	1.440 (8)
Ta-N(33)	2.165 (5)	N(33)-C(32)	1.286 (8)
Ta-C(21)	2.187 (7)	N(33)-C(34)	1.429 (8)
Ta-C(32)	2.200 (6)		
O(2)-Ta-O(11)	175.0 (2)	O(11)-Ta-N(22)	90.3 (2)
On2)-Ta-N(22)	90.2 (2)	O(11)-Ta-N(33)	90.7 (2)
O(2)-Ta-N(33)	88.9 (2)	O(11)-Ta-C(21)	86.9 (2)
O(2)-Ta-C(21)	90.6 (2)	O(11)-Ta-C(32)	88.5 (2)
O(2)-Ta-C(32)	88.3 (2)	O(11)-Ta-C(42)	91.8 (2)
O(2)-Ta-C(42)	93.2 (2)	N(22)-Ta-N(33)	179.0 (2)
N(33)-Ta-C(21)	146.1 (2)	N(22)-Ta-C(21)	34.4 (2)
N(33)-Ta-C(32)	34.3 (2)	N(22)-Ta-C(32)	146.1 (2)
N(33)-Ta-C(42)	90.9 (2)	N(22)-Ta-C(42)	88.6 (2)
Ta-O(2)-C(3)	168.8 (4)	C(21)-Ta-C(32)	111.8 (2)
Ta-O(11)-C(12)	168.3 (4)	C(21)-Ta-C(42)	122.9 (3)
Ta-N(22)-C(21)	74.3 (4)	C(32)-Ta-C(42)	125.2 (3)
Ta-C(21)-N(22)	71.3 (4)	Ta-N(33)-C(32)	74.4 (4)
		Ta-C(32)-N(33)	71.4 (4)

In solution all of compounds VI exhibit spectra and fluxionality consistent with the maintenance of a structure in solution similar to that observed for VIa in the solid state. It can be seen from Figure 9 that the arrangement of the aryl ring of the 2,6-dimethylphenoxide ligands is such that two nonequivalent methyl groups results: those lying roughly over the $Ta\text{-}CH_3$ group and those lying away. The solution ^1H NMR spectra of derivatives VI indeed show these methyl groups as two separate singlets of equal intensity, indicating that rotation about the Ta–O–Ar bonds is restricted. On warming solutions of the xylyl isocyanide derivatives VIa and VIc, these signals collapse and coalesce into a single peak at higher temperatures. Activation energies $\Delta G^{\ddagger}$ at coalescence temperatures T_c (parentheses) can be estimated as 13.1 ± 0.5 kcal mol^{-1} (-20 °C) for VIa and 16.1 ± 0.5 kcal mol^{-1} (+35 °C) for VIc. The higher rotational barrier for the benzyl complex over its methyl counterpart can be attributed to steric effects. The use of the sterically very demanding 2,6-diisopropylphenyl isocyanide (isoNC) leads to the derivatives VIb and VId (Scheme III). Here the nonequivalent aryloxide methyl groups remain as separate sharp singlets even up to 60 °C where the complexes begin to undergo thermolysis. Furthermore, the $CHMe_2$ groups of the η^2-isoNCR ligand are diastereotopic, indicating significant restriction of the rotation of the 2,6-diisopropylphenyl group in these very crowded molecules.

Coordination Properties of the η^2-Iminoacyl Ligand. Some of the observed reactivity of early transition metal, actinide and lanthanide η^2-acyl groups is normally ascribed to the presence of significant oxy–carbenoid character to the functionality.[9,10] A related amido–carbene resonance can be envisioned for the isoelectronic η^2-iminoacyl group, particularly in view of the fact that intramolecular coupling reactions can also take place to produce ene-diamide ligands.[22b] However, Hoffman et al. have indicated that the observed reactivity of η^2-acyl groups is a function of a low-lying LUMO consisting of the acyl π^*CO pushed down in energy by empty d orbitals of correct symmetry on the metal.[11] This low-lying π^* orbital accounts for the observed electrophilic character of the η^2-acyl carbon without invoking an oxy–carbene resonance. The structural data we have obtained allows us to more thoroughly characterize the coordination properties of η^2-iminoacyl groups bound to early transition metals and to compare them with

Table XII. Selected Structural Data on Transition-Metal Iminoacyl Derivatives

complex	M—C=N, Å	M—N=C, Å	C=N, Å	L(M—C=N), deg	[d(M—N) − d(M—C)]	ref
Ia	2.096 (5)	2.015 (4)	1.257 (6)	75.8 (3)	−0.081 (7)	*a*
Ib	2.086 (6)	2.025 (5)	1.279 (7)	74.5 (3)	−0.061 (8)	*a*
IId	2.228 (3)	2.221 (3)	1.286 (4)	72.9 (2)	−0.003 (5)	*a*
IIg	2.209 (6)	2.212 (5)	1.275 (8)	73.4 (4)	+0.003 (8)	*a*
IVa	2.241 (3)	2.211 (3)	1.277 (4)	72.0 (2)	−0.030 (5)	*a*
	2.249 (4)	2.257 (3)	1.284 (4)	73.8 (2)	+0.008 (6)	
	2.251 (3)	2.248 (3)	1.276 (4)	73.4 (2)	−0.003 (5)	
VIa	2.187 (7)	2.151 (5)	1.281 (8)	71.3 (4)	−0.036 (8)	*a*
	2.200 (6)	2.165 (5)	1.286 (8)	71.4 (4)	−0.035 (7)	
$[HB(3,5\text{-}Me_2Bz)_3]Zr(O\text{-}t\text{-}Bu)(\eta^2\text{-}NCMe)Me$	2.20 (1)	2.194 (8)	1.27 (2)	72.8 (6)	−0.006 (15)	18b
$CpTa(\eta^2\text{-}t\text{-}BuNCMe)(ArCCAr)Me$	2.10 (1)	2.12 (1)	1.25 (1)		+0.02 (2)	15c
$Cp_2Ti(\eta^2\text{-}xyNCPh)$	2.096 (4)	2.149 (4)	1.280 (6)	74.7 (2)	+0.053 (7)	16a
$Cp_3U(\eta^2\text{-}cyNCMe)$	2.36 (2)	2.40 (2)	1.25 (2)		+0.04 (3)	18a
$CpMo(CO)_2(\eta^2\text{-}PhNCMe)$	2.106 (5)	2.143 (4)	1.233 (6)	71.5 (3)	+0.037 (8)	19a
$CpMo(CO)_2(P(OMe)_3)(\eta^1\text{-}PhNCMe)$	2.27 (1)	3.06 (1)	1.266 (9)	116.9 (7)	+0.79 (2)	19a

[a] This work

their isoelectronic η^2-acyl counterparts.

Table XII contains some relevant structural parameters for the molecules obtained in this study along with data for some other iminoacyl compounds reported in the literature. Iminoacyl and iminoformyl groups have also been observed to bridge two or even three metal centers[17b,20a,b] but the structural data on this type of bonding have not been included in Table XII for comparison. Possibly the easiest parameter to evaluate is the C–N distance. For the compounds obtained in this study this distance varies from 1.257 (6) Å in Ia to 1.286 (4) Å for the η^2-iminoacyls of IId. These values are comparable to those found for other η^2- and η^1-iminoacyl functions. Typical carbon–nitrogen single (amines), double (imines), and triple (alkyl isocyanides) bonds lie in the region of 1.47, 1.28, and 1.16 Å, respectively. Hence, this structural parameter for the η^2-iminoacyl appears consistent with the presence of a carbon–nitrogen double bond. This apparently implies little ground state structural contribution from an amido–carbene resonance, although the C–N distance in Fischer amido–carbenes lies close to 1.31 Å,[26] a distance slightly shorter than the C–O distance found in alkoxy–carbene complexes. This is due to the considerable nitrogen-to-carbon π-donation that can take place resulting in a partial double bond.[26] The value of C–O distances in related η^2-acyl compounds ranges from 1.18 (2) to 1.30 (2) Å.[6]

The M–C and M–N distances prove to be an interesting structural feature of these compounds. In the case of the known η^2-acyl complexes the value of [d(M–O)–d(M–C)acyl] and the M–C–O(acyl) angle have been shown to fall with the increasing oxophilicity of the metal center.[6,8b] The difference in the metal distances to the oxygen and carbon atoms varies from 0.44 to −0.07 Å. Table XII lists the corresponding parameter for the η^2-iminoacyl complexes. Of the nine iminoacyl ligands structurally studied in this work it can be seen that the M–C and M–N distances are essentially identical. The M–C distances are comparable to the distances found for alkyl groups bound to similar metal centers. This is highlighted in the structures of Ia, Ib, and VIa where noninserted, terminal alkyl groups remain. In the case of the η^2-acyl $Cp_2Zr(\eta^2\text{-}MeCO)(Me)$ the Zr–C(acyl) distance of 2.197 (6) Å was considerably shorter than the Zr–CH_3 distance of 2.336 (7) Å.[5] Similarly a preliminary report of the structure of the complex $Cp_2Zr(\eta^2\text{-}Ph_2CHC{=}NMe)(Me)$ gave values of Zr–C(iminoacyl) of 2.247 (5) Å and Zr–CH_3 of 2.336 (7) Å.[27] Hence in these zirconocene derivatives the difference in the metal–carbon distance to η^2-RCX (X = O, NR′) and alkyl groups appears much more pronounced than for the aryloxide derivatives in this study. The metal–nitrogen distances to the iminoacyl groups are significantly shorter than the distance found for pyridine ligands bound to the same metal centers. Hence we can compare the Ti–N distance of 2.02 Å (av) found for Ia and Ib with the Ti–NC_5H_5 distance of 2.293 (5) Å in the cyclometalated complex $Ti(OC_6H_3\text{-}t\text{-}BuMe_2CH_2)(OAr2,6\text{-}t\text{-}Bu_2)(CH_2SiMe_3)(NC_5H_5)$.[23b] Similarly the Zr–N distances in IId and IVa of 2.211 (3)–2.257 (3) Å and the Hf–N distance of 2.212 (5) Å in IIg can be compared to the Zr–NC_5H_5 distance of 2.403 (1) Å in $Cp_2Zr(\eta^2\text{-}H_2C{=}CO)(py)$[28] and 2.374 (4) Å in $Hf(OAr\text{-}2,6\text{-}t\text{-}Bu_2)_2(CH_2pyMe)_2$[29] ($CH_2pyMe$ = C, N-bound (2-(6-methylpyridyl))methyl). Although shorter than these simple dative bonds, the M–N (iminoacyl) distances are still longer than the corresponding distance to terminal dialkyl–amido ligands. Compare the M–N distance in the series $MCl(N(SiMe_3)_2)_3$: M = Ti, 1.94 (1) Å, Zr, 2.070 (3) Å, and Hf, 2.04 (1) Å.[30] A very informative comparison is between the η^2-iminoacyl groups studied here and a tungstacyclopropane complex, $W(\eta^2\text{-}t\text{-}BuNCMe_2)(=N\text{-}t\text{-}Bu)(N(t\text{-}Bu)CMe{=}CMe_2)(CH_3)$, structurally characterized by Wilkinson and co-workers.[15a] Here the C–N distance of 1.44 (2) Å is totally consistent with the presence of a single bond while W–N and W–C distances of 1.19 (1) and 2.20 (1) Å are typical of those to terminal tungsten amido and alkyl groups.

The initial impact of the structural data obtained in this study is to imply little contribution to the ground state of an amido–carbene resonance form for these η^2-iminoacyl ligands. This is

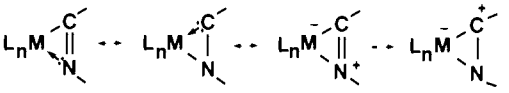

based on the short C–N distances and the M–N distance being somewhat longer than that predicted for a metal–amido bond. The π-donor ability of the nitrogen atom in these ligands complicates this simple picture. However, the structural data can be accommodated very well into the charged resonance picture shown in which the electron deficient metal has strongly polarized the metal–iminoacyl bonding.

Experimental Section

All operations were carried out under a dry nitrogen atmosphere either in a Vacuum Atmospheres dri-lab or by standard Schlenck techniques. Hydrocarbon solvents were dried by distillation from sodium benzophenone under a nitrogen atmosphere. 2,6-Dimethylphenyl isocyanide (xyNC) was purchased (Fluka A.G.) while *t*-BuNC, PhNC, and 2,6-diisopropylphenyl isocyanide (isoNC) were synthesized by literature methods. The alkyls $Zr(OAr\text{-}2,6\text{-}t\text{-}Bu_2)_2(CH_2Ph)_2$, $Zr(OAr\text{-}2,6\text{-}t\text{-}Bu_2)(CH_2Ph)_3$, $Ta(OAr\text{-}2,6\text{-}Me_2)_3(CH_2Ph)_2$, $Ta(OAr\text{-}2,6\text{-}Me_2)_2(CH_2Ph)_3$, and $Ta(OAr\text{-}2,6\text{-}Me_2)_2(CH_3)_3$ were obtained by published methods,[23] as were $Ti(OAr\text{-}2,6\text{-}i\text{-}Pr_2)_2(CH_2Ph)_2$, $Ti(OAr\text{-}2,6\text{-}Ph_2)_2(CH_2Ph)_2$, $Ti(OAr\text{-}2,6\text{-}Ph_2)_2(CH_2SiMe_3)_2$, and $M(OAr\text{-}2,6\text{-}t\text{-}Bu_2)_2(CH_3)_2$ (M = Zr, Hf).[23d] ^1H and ^{13}C NMR spectra were recorded either

(26) Cardin, D. J.; Cetinkaya, B.; Doyle, M. J.; Lappert, M. J. *Chem. Soc. Rev.* **1973**, *2*, 99.

(27) Bristow, G. S.; Lappert, M. F.; Atwood, J. L.; Hunter, W. E., unpublished work cited in the following: *Comprehensive Organometallic Chemistry*; Wilkinson, G. W., Stone, F. G. A., Abel, K. W., Eds.; Pergamon: Oxford, 1982; Chapter 23, p 600.

(28) Moore, K. J.; Straus, D. A.; Armantrout, J.; Santarsiero, B. D.; Grubbs, R. H.; Bercaw, J. E. *J. Am. Chem. Soc.* **1983**, *105*, 2068.

(29) Beshouri, S. M.; Rothwell, I. P., unpublished results.

(30) Airoldi, C.; Bradley, D. C.; Chudzynska, H.; Hursthouse, M. B.; Abdul-Malik, K. M.; Praisthloy, P. R. *J. Chem. Soc., Dalton Trans.* **1980**, 2010.

on a Varian Associates XL-200 spectrometer or also on a Nicolet Instruments 470 MHz instrument.

Because of the similarity of the synthetic procedures used to obtain each of the η^2-iminoacyl compounds I–VI, only one representative synthesis will be outlined in detail for each type. Full analytical and spectroscopic data will, however, be reported.

Mono-Iminoacyl Derivatives (I). Synthesis of Ti(OAr-2,6-*i*-Pr_2)$_2$(η^2-*t*-BuNCCH$_2$Ph)(CH$_2$Ph) (Ia). To a solution of Ti(OAr-2,6-*i*-Pr_2)$_2$(CH$_2$Ph)$_2$ (300 mg) in hexane (20 mL) was slowly added *t*-BuNC (45 mg) also in hexane (5 mL). The initially deep-red solution immediately became orange, and after a few minutes orange-yellow crystals began to form. The reaction mixture was allowed to stand for 1 h before the yellow solution was decanted off the crystalline product. Yield = 280 mg (81%). More of the product was obtained on cooling the mother liquor to −15 °C. Compounds Ib and Ic were both found to crystallize with 0.5 molecule of hexane.

Ia: Anal. Calcd for $TiC_{43}H_{57}NO_2$: C, 77.33; H, 8.60; N, 2.01. Found: C, 77.31; H, 8.75, N, 2.01. ^{1}H NMR (C_6D_6, 30 °C) δ 3.20 (s, TiCH_2Ph), 4.22 (s, *t*-BuNCCH_2Ph), 1.15 (s, *t-Bu*-NCCH$_2$Ph), 3.35 (sp, C*H*Me$_2$), 1.20, 1.33 (d, CH*Me*$_2$), 6.8–7.2 (m, aromatics). ^{13}C NMR (C_6D_6, 30 °C) δ 63.2 (TiCH$_2$Ph), 41.3 (*t*-BuNCCH$_2$Ph), 230.5 (*t*-BuN*C*CH$_2$Ph), 62.5 (N*C*Me$_3$), 30.7 (NC(*C*H$_3$)$_3$), 26.2 (*C*HMe$_2$), 23.1, 23.76 (CH(*C*H$_3$)$_2$).

Ib: Anal. Calcd for $TiC_{54}H_{60}NO_2Si_2$: C, 75.48; H, 7.02, N, 1.16. Found: C, 74.81; H, 7.06; N, 1.38. ^{1}H NMR (C_6D_6, 30 °C) δ 0.70 (s, TiCH_2SiMe$_3$), 2.51 (s, PhNCCH_2SiMe$_3$), −0.18, −0.39 (s, Si*Me*$_3$), 6.2–7.5 (m, aromatics). ^{13}C NMR (C_6D_6, 30 °C) δ 71.1 (TiCH$_2$SiMe$_3$), 29.1 (PhNCCH$_2$SiMe$_3$), 240.7 (PhN*C*CH$_2$SiMe$_3$), 0.1, 2.7 (Si*Me*$_3$).

Ic: Anal. Calcd for $TiSi_2C_{56}H_{64}NO_2$: C, 75.81; H, 7.29; N, 1.58. Found: C, 75.33; H, 7.36; N, 1.21. ^{1}H NMR (C_6D_6, 30 °C) δ 0.63 (s, TiCH_2SiMe$_3$), 2.30 (s, xyNCCH_2SiMe$_3$), 1.08 (s, xyCH$_3$), −0.80, −0.30 (s, Si*Me*$_3$), 6.7–7.6 (m, aromatics). ^{13}C NMR (C_6D_6, 30 °C) δ 71.8 (TiCH$_2$SiMe$_3$), 30.2 (xyNCCH$_2$SiMe$_3$), 232.3 (xyN*C*CH$_2$SiMe$_3$), 18.2 (xy*C*H$_3$), 0.05, 2.65 (Si*Me*$_3$).

Id: Anal. Calcd for $TiC_{59}H_{49}NO_2$: C, 83.2; H, 5.80; N, 1.64. Found: C, 80.20; H, 5.59; N, 1.04. ^{1}H NMR (C_6D_6, 30 °C) δ 2.01 (s, TiCH_2Ph), 3.05 (s, xyNCCH_2Ph), 0.86 (s, xy*C*H$_3$), 6.4–7.5 (m, aromatics). ^{13}C NMR (C_6D_6, 30 °C) δ 76.3 (TiCH$_2$Ph), 41.7 (xyNCCH$_2$Ph), 18.2 (xy*C*H$_3$), 238.9 (xyN*C*CH$_2$Ph).

Ie: Anal. Calcd for $ZrC_{51}H_{65}NO_2$: C, 75.13; H, 8.04; N, 1.72. Found: C, 75.08; H, 8.20; N, 1.79. ^{1}H NMR (C_6D_6, 30 °C) δ 3.14 (s, ZrCH_2Ph), 4.00 (s, xyNCCH_2Ph), 1.68 (s, xy*C*H$_3$), 1.47 (s, C*Me*$_3$), 6.6–7.3 (m, aromatics). ^{13}C NMR (C_6D_6, 30 °C) δ 65.8 (ZrCH$_2$Ph), 44.4 (xyNCCH$_2$Ph), 246.3 (xyN*C*CH$_2$Ph), 18.0 (xy*C*H$_3$), 35.2 (*C*Me$_3$), 31.8 (C(*C*H$_3$)$_3$).

Bis-Iminoacyl Derivatives (II). Synthesis of Zr(OAr-2,6-*t*-Bu_2)$_2$(xyNCCH$_3$)$_2$ (IIe). To a solution of Zr(OAr-2,6-*t*-Bu_2)$_2$(CH$_3$)$_2$ (520 mg) in hexane (20 mL) was added 2,6-dimethylphenyl isocyanide (xyNC, 300 mg) in toluene (5 mL). The resulting mixture was allowed to stand for 1 h before being cooled to −15 °C whereupon bright yellow crystals of product were given. Yield = 600 mg (67%). Evaporation of the mother liquor and analysis of the residue by ^{1}H NMR showed mainly IIe with some HOAr-2,6-*t*-Bu_2.

IIa: Anal. Calcd for $TiC_{56}H_{66}N_2O_2$: C, 79.39; H, 7.87; N, 3.31. Found: C, 79.55; H, 7.82; N, 3.11. ^{1}H NMR (C_6D_6, 30 °C) δ 3.75 (s, xyNCCH$_2$Ph), 2.10 (s, xy*C*H$_3$), 3.65 (sp, C*H*Me$_2$), 1.30 (d, CH(*C*H$_3$)$_2$), 6.8–7.2 (m, aromatics). ^{13}C NMR (C_6D_6, 30 °C) δ 43.8 (xyNCCH$_2$Ph), 237.1 (xyN*C*CH$_2$Ph), 18.7 (xy*C*H$_3$), 25.7 (*C*HMe$_2$), 24.1 (CH(*C*H$_3$)$_2$).

IIb: Anal. Calcd for $TiC_{68}H_{58}N_2O_2$: C, 83.08, H, 5.95; N, 2.85. Found: C, 83.26; H, 5.97; N, 2.71. ^{1}H NMR (C_6D_6, 30 °C) δ 2.79 (s, xyNCCH_2Ph), 1.50 (s, xy*C*H$_3$), 6.3–7.6 (m, aromatics). ^{13}C NMR (C_6D_6, 30 °C) δ 43.3 (xyNCCH$_2$Ph), 20.4 (xy*C*H$_3$).

IIc: Anal. Calcd for $ZrC_{60}H_{74}N_2O_2$: C, 76.14; H, 7.88; N, 3.00. Found: C, 75.4; H, 8.08; N, 3.16. ^{1}H NMR (C_6D_6, 30 °C) δ 4.21 (s, xyNCCH_2Ph), 1.68 (s, xy*C*H$_3$), 1.35 (s, *t-Bu*), 6.7–7.3 (m, aromatics). ^{13}C NMR (C_6D_6, 30 °C) δ 43.1 (xyNCCH$_2$Ph), 239.0 (xyN*C*CH$_2$Ph), 18.9 (xy*C*H$_3$), 35.1 (*C*Me$_3$), 32.4 (C(*C*H$_3$)$_3$).

IId: Anal. Calcd for $ZrC_{52}H_{74}N_2O_2$: C, 71.91; H, 8.86; N, 3.00. Found: C, 73.34; H, 8.68; N, 3.26. ^{1}H NMR (C_6D_6, 30 °C) δ 4.30 (s, *t*-BuNCCH_2Ph), 0.97 (*t-Bu*NCCH$_2$Ph), 1.55 (OAr-*t*-Bu), 6.8–7.4 (m, aromatics). ^{13}C NMR (C_6D_6, 30 °C) δ 41.1 (*t*-BuNCCH$_2$Ph), 244.3 (*t*-BuN*C*CH$_2$Ph), 61.2 (N*C*Me$_3$), 30.1 (NC(*C*H$_3$)$_3$), 35.7 (OAr*C*Me$_3$), 32.9 (OArC(*C*H$_3$)$_3$).

IIe: Anal. Calcd for $ZrC_{48}H_{66}N_2O_2$: C, 72.59; H, 8.38; N, 3.53. Found: C, 73.09; H, 8.37; N, 3.28. ^{1}H NMR (C_6D_6, 30 °C) δ 2.21 (s, xyNCCH_3), 1.73 (s, xy*C*H$_3$), 1.53 (s, *t*-Bu), 6.8–7.4 (m, aromatics). ^{13}C NMR (C_6D_6, 30 °C) δ 24.2 (xyNCCH_3), 245.2 (xyN*C*CH$_3$), 19.3 (xy*C*H$_3$), 35.7 (*C*(CH$_3$)$_3$), 32.4 (C(*C*H$_3$)$_3$).

IIf: Anal. Calcd for $ZrC_{44}H_{58}N_2O_2$: C, 71.59, H, 7.92; N, 3.79. Found: C, 70.46; H, 8.21; N, 3.61. ^{1}H NMR (C_6D_6, 30 °C) δ 2.22 (s, PhNCCH_3), 1.62 (s, OAr-*t-Bu*), 6.4–7.3 (m, aromatics). ^{13}C NMR (C_6D_6, 30 °C) δ 21.8 (PhNCCH_3), 236.4 (PhN*C*CH$_3$), 35.3 (*C*(CH$_3$)$_3$), 32.4 (C(*C*H$_3$)$_3$).

IIg: Anal. Calcd for $HfC_{44}H_{58}N_2O_2$: C, 64.02; H, 7.08; N, 3.39. Found: C, 64.10; H, 7.37; N, 3.21. ^{1}H NMR (C_6D_6, 30 °C) δ 2.25 (s, PhNCCH_3), 1.70 (s, OAr-*t-Bu*), 6.7–7.3 (m, aromatics). ^{13}C NMR (C_6D_6, 30 °C) δ 23.1 (PhNCCH_3), 255.0 (PhN*C*CH$_3$), 31.6 (*C*(CH$_3$)$_3$, 35.5 (C(*C*H$_3$)$_3$.

Synthesis of Zr(OAr-2,6-*t*-Bu_2)(η^2-xyNCCH$_2$Ph)$_2$(CH$_2$Ph) (III). The slow addition of xyNC (2 equiv) in benzene to a dilute benzene solution of Zr(OAr-2,6-*t*-Bu_2)(CH$_2$Ph)$_3$ led to a dark brown solution. Removal of solvent led to the crude product as a brownish-yellow solid, which was washed with hexane. The product was found to be thermally unstable over hours in solution and so no attempt at recrystallization was made. Anal. Calcd for $ZrC_{53}H_{60}N_2O$: C, 76.49; H, 7.27; N, 3.37. Found: C, 75.49; H, 7.17; N, 3.14. ^{1}H NMR (C_6D_6, 30 °C) δ 3.69 (d), 3.76 (d, xyNCCH_2Ph), 2.94 (s, ZrCH_2Ph), 2.13 (s, xy*C*H$_3$), 1.44 (s, OAr-*t*-Bu), 6.6–7.4 (m, aromatics). ^{13}C NMR (C_6D_6, 30 °C) δ 253.1 (xyN*C*CH$_2$Ph), 60.1 (ZrCH_2Ph), 42.9 (xyNC*C*H$_2$Ph), 18.4 (xy*C*H$_3$), 35.1 (*C*Me$_3$), 31.9 (C(*C*H$_3$)$_3$).

Tris-Iminoacyl Derivatives (IV). Synthesis of Zr(OAr-2,6-*t*-Bu_2)(*t*-BuNCCH$_2$Ph)$_3$ (IVa). The addition of *t*-BuNC (≥3 equiv) from a syringe to a hexane solution of Zr(OAr-2,6-*t*-Bu_2)(CH$_2$Ph)$_3$ (500 mg) in hexane (25 mL) led to a pale yellow solution, from which colorless crystals of product were deposited on slow cooling. Yields were typically 60–80%.

IVa: Anal. Calcd for $ZrC_{50}H_{69}N_3O$: C, 73.30; H, 8.49; N, 5.13. Found: C, 73.37; H, 8.23; N, 5.14. ^{1}H NMR (C_6D_6, 30 °C) δ 4.25 (*t*-BuNCCH_2Ph), 1.08 (*t-Bu*NCCH$_2$Ph), 1.42 (OAr-*t-Bu*), 7.0–7.3 (m, aromatics). ^{13}C NMR (C_6D_6, 30 °C) δ 40.8 (*t*-BuNCCH$_2$Ph), 239.6 (*t*-BuN*C*CH$_2$Ph), 58.6 (N*C*Me$_3$), 30.1 (NC(*C*H$_3$)$_3$), 35.6 (OAr*C*Me$_3$), 32.4 (OArC(*C*H$_3$)$_3$).

IVb: Anal. Calcd for $ZrC_{62}H_{69}N_3O$: C, 77.29; H, 7.22; N, 4.36. Found: C, 70.00; H, 6.67; N, 3.90. ^{1}H NMR ($C_5D_5CD_3$, −48 °C) δ 3.38 (s), 3.71 (d), 4.20 (d, xyNCCH_2Ph), at 30 °C only one type of xyCH$_3$ at δ 1.85 and one type of OAr-*t-Bu* at δ 1.47 were observed. However, on cooling these split into five peaks presumably due to restricted rotation of these alkyl groups. Chemical shifts at −48 °C, δ 1.32, 1.47, 1.50, 1.53, 2.00. ^{13}C NMR ($C_6D_5CD_3$, −40 °C) δ 247.1, 262.3 (xyN*C*CH$_2$Ph). No attempt was made to assign the other peaks.

Synthesis of Ta(OAr-2,6-Me$_2$)$_3$(xyNCCH$_2$Ph)$_2$ (V). To a solution of Ta(OAr-2,6-Me$_2$)$_3$(CH$_2$Ph)$_2$ (250 mg) in hexane (20 mL) was added solid xyNC (110 mg, 2 equiv) rapidly. After the mixture was stirred for 2 h the precipitated product was filtered, washed with hexane, and dried. Yield = 310 mg (91%). Anal. Calcd for $TaC_{56}H_{59}N_2O_3$: C, 68.01; H, 6.01; N, 2.83. Found: C, 67.21; H, 6.06, N, 2.81. ^{1}H NMR (C_6D_6, 30 °C) δ 4.63 (s, xyNCCH_2Ph), 2.28 (s, xy*C*H$_3$), 2.28 (s, OAr*C*H$_3$), 6.8–7.4 (m, aromatics). ^{13}C NMR (C_6D_6, 30 °C) δ 45.3 (xyNCCH$_2$Ph), 241.7 (xyN*C*CH$_2$Ph), 17.5, 18.0 (xy*C*H$_3$ and OAr*C*H$_3$).

Bis-Iminoacyl Derivatives (VI). Synthesis of Ta(OAr-2,6-Me$_2$)$_2$(η^2-xyNCCH$_3$)$_2$(CH$_3$) (VIa). To a solution of Ta(OAr-2,6-Me$_2$)$_2$(CH$_3$)$_3$ (500 mg) in hexane (20 mL) was added xyNC (280 mg) also in hexane (15 mL). After the mixture was stirred for 5 min the product was formed as a white precipitate which was filtered and recrystallized from toluene/hexane as large colorless blocks. Yield = 230 mg (30%).

VIa: Anal. Calcd for $TaC_{37}H_{45}N_2O$: C, 60.82; H, 6.20; N, 3.83. Found: C, 60.28; H, 6.31; N, 3.54. ^{1}H NMR ($C_6D_5CD_3$, −40 °C) δ 1.57 (s, TaCH_3), 2.48 (s, xyNCCH_3), 1.78 (s, xyCH_3), 2.37, 2.46 (s, OAr*C*H$_3$), 6.9–7.2 (m, aromatics). ^{13}C NMR (C_6D_6, 30 °C) δ 22.3 (Ta*C*H$_3$), 21.2 (xyNCCH_3), 239.6 (xyN*C*CH$_3$), 17.6, 17.7 (xy*C*H$_3$ and OAr*C*H$_3$).

VIb: Anal. Calcd for $TaC_{45}H_{61}O_2N_2$: C, 64.13; H, 7.29; N, 3.32. Found: C, 64.23; H, 7.93; N, 3.09. ^{1}H NMR (C_6D_6, 30 °C) δ 1.69 (s, TaCH_3), 2.67 (s, isoNCCH_3), 2.42, 2.37 (s, OAr*C*H$_3$), 2.78 (sp, iso*C*HMe$_2$), 0.65, 1.08 (d, isoCH*Me*$_2$). ^{13}C NMR (C_6D_6, 30 °C) δ 19.2 (Ta*C*H$_3$), 22.4 (isoNCCH_3), 240.8 (isoN*C*CH$_3$), 23.1, 23.8 (OAr*C*H$_3$, iso*C*H$_3$).

VIc: Anal. Calcd for $TaC_{55}H_{57}N_2O_2$: C, 68.89; H, 5.98; N, 2.91. Found: C, 68.26; H, 6.01; N, 2.83. ^{1}H NMR ($C_6D_5CD_3$, 18 °C) δ 3.71 (s, TaCH_2Ph), 4.25 (s, xyNCCH_2Ph), 2.35, 2.39 (s, OAr*C*H$_3$), 1.77 (s, xyCH_3), 6.8–7.3 (m, aromatics). ^{13}C NMR ($C_6D_5CD_3$, 30 °C) 51.5 (Ta*C*H$_2$Ph), 41.8 (xyNCCH$_2$Ph), 239.7 (xyN*C*CH$_2$Ph), 17.61, 17.65 (xy*C*H$_3$, OAr*C*H$_3$).

VId: Anal. Calcd for $TaC_{63}H_{73}N_2O_2$: C, 70.64; H, 6.86; N, 2.61. Found: C, 70.70; H, 7.05; N, 2.72. ^{1}H NMR ($C_6D_5CD_3$, 30 °C): 3.95 (s, TaCH_2Ph), 4.38 (s, isoNCCH_2Ph), 1.98, 2.49 (s, OAr*C*H$_3$), 2.73 (sp, iso*C*HMe$_2$), 0.72, 1.02 (d, isoCH*Me*$_2$), 6.7–7.4 (m, aromatics). ^{13}C NMR (C_6D_6, 30 °C) δ 53.3 (Ta*C*H$_2$Ph), 44.5 (isoNCCH$_2$Ph), 240.1 (isoN*C*CH$_2$Ph).

Table XIII. Crystal Structure Determination Data

	Ia	Ib		Ia	Ib
formula	$TiC_{43}H_{57}NO_2$	$TiC_{51}H_{53}NSi_2O_2 \cdot 1/2C_6H_4$	linear abs coeff, cm^{-1}	2.509	2.601
fw	667.83	859.15	temp, deg C	−154	−160
space group	$P\bar{1}$	$P\bar{1}$	detector aperture	3.0 mm wide × 4.0 mm high	
a, Å	18.678 (7)	23.086 (9)	takeoff angle, deg	2.0	
b, Å	11.724 (4)	11.100 (4)	scan speed, deg/min	6.0	4.0
c, Å	9.953 (3)	10.122 (3)	scan width, deg	1.6 + dispersion	2.0 + dispersion
α, deg	111.99 (2)	95.94 (2)	bkgd counts, s	8	8
β, deg	74.23 (2)	107.38 (2)	2θ range, deg	6–45	6–45
γ, deg	101.96 (2)	78.51 (2)	unique data	5082	6330
Z	2	2	unique data with $F_o > 3.00\sigma(F)$	3663 (2.33σ)	4441
V, $Å^3$	1931	2423	$R(F)$	0.0692	0.0685
density (calcd), g/cm^3	1.148	1.178	$R_w(F)$	0.0724	0.0644
crystal size, mm	0.50 × 0.50 × 0.50	0.24 × 0.24 × 0.30	goodness of fit	1.009	1.111
crystal color	yellow orange	yellow	largest Δ/σ	0.05	0.05
radiation	Mo Kα (λ = 0.71069 Å)				

	IId	IIg		IId	IIg
formula	$ZrC_{52}H_{74}N_2O_2$	$HfC_{44}H_{58}N_2O_2$	temp, deg C	−157	+22
fw	850.39	825.46	detector aperture	3.0 mm wide × 4.0 mm high	(1.5 + tan θ) mm wide × 4.0 mm high
space group	$C2/c$	$C2/c$			
a, Å	23.612 (8)	13.203 (3)	takeoff angle, deg	2.0	4.90
b, Å	11.198 (4)	15.150 (3)	scan speed, deg/min	4.0	variable
c, Å	21.243 (8)	21.213 (6)	scan width, deg	2.0 + dispersion	0.8 + 0.35 tan θ 50% of scan time
α, deg					
β, deg	123.52 (2)	103.33 (2)	bkgd counts, s	8	
γ, deg			2θ range, deg	6–45	4–50
Z	4	4	unique data	3066	3769
V, $Å^3$	4682	4129	unique data with $F_o > 3.00\sigma(F)$	2665	2726
density (calcd), g/cm^3	1.206	1.328			
crystal size, mm	0.15 × 0.15 × 0.18	0.20 × 0.20 × 0.17	$R(F)$	0.0345	0.0360
crystal color	colorless	yellow	$R_w(F)$	0.0367	0.0470
radiation	Mo Kα (λ = 0.71069 Å)		goodness of fit	0.813	0.976
linear abs coeff, cm^{-1}	2.680	25.38	largest Δ/σ	0.05	0.02

	IVa	VIa		IVa	VIa
formula	$ZrC_{50}H_{69}N_3O$	$TaC_{37}H_{45}N_2O_2$	linear abs coeff, cm^{-1}	2.751	33.100
fw	819.33	730.72	temp, deg C	−155	−160
space group	$P\bar{1}$	$P\bar{1}$	detector aperture	3 mm wide × 4 mm high	
a, Å	14.031 (5)	10.881 (2)	takeoff angle, deg	2.0	
b, Å	15.788 (7)	18.154 (5)	scan speed, deg/min	4.0	
c, Å	10.918 (4)	9.188 (2)	scan width, deg	1.8 + dispersion	2.0 + dispersion
α, deg	108.89 (2)	99.07 (1)	bkgd counts, s	8	6
β, deg	97.01 (2)	108.80 (1)	2θ range, deg	6–45	6–45
γ, deg	94.30 (2)	75.36 (1)	unique data	5904	4358
Z	2	2	unique data with $F_o > 3.00\sigma(F)$	5031	3923
V, $Å^3$	2254	1657			
density (calcd), g/cm^3	1.207	1.465	$R(F)$	0.0456	0.0323
crystal size, mm	0.20 × 0.17 × 0.28	0.12 × 0.10 × 0.10	$R_w(F)$	0.0477	0.0327
crystal color	colorless	yellow	goodness of fit	0.985	0.738
radiation	Mo Kα (λ = 0.71069 Å)		largest Δ/σ	0.05	0.05

Crystallographic Studies. Five of the six structure determinations were obtained through the Molecular Structure Center of Indiana University[31] while the sixth, that of IIg, was done in house.[32] Crystal parameters are given in Table XIII.

Ti(OAr-2,6-*i*-Pr_2)$_2$(η^2-*t*-BuNCCH$_2$Ph)(CH$_2$Ph) (Ia). A suitable crystal was located and transferred to the goniostat with use of standard inert atmosphere handling techniques employed by the IUMSC[31] and cooled to −154 °C for characterization and data collection.

A systematic search of a limited hemisphere of reciprocal space located a set of diffraction maxima with no systematic absences or symmetry, indicating a triclinic space group. Subsequent solution and refinement confirmed the space group to be $P\bar{1}$.

The structure was solved by a combination of direct methods (MULTAN78) and Fourier techniques and refined by full-matrix least squares. Many of the hydrogen atom positions were visible in difference Fourier phases on the non-hydrogen parameters. The positions of all hydrogens were calculated and placed in fixed idealized d(C–H) = 0.95 Å for the final cycles. The hydrogen atoms were assigned a thermal parameter of 1 + B_{iso} of the carbon atom to which they were bound. All were fixed with the exception of those on the benzyl. These were refined to confirm the positions and then fixed in the final cycle.

A final difference Fourier was essentially featureless, with the largest peak being 0.50 e/Å^3. No absorption correction was performed.

Ti(OAr-2,6-Ph_2)$_2$(η^2-PhNCCH$_2$SiMe$_3$)(CH$_2$SiMe$_3$)·$^1/_2$C$_6$H$_{14}$ (Ib). A suitable crystal was located and transferred to the goniostat with use of standard inert atmosphere handling techniques employed by the IUMSC and cooled to −160 °C for characterization and data collection.

A systematic search of a limited hemisphere of reciprocal space located a set of diffraction maxima with no systematic absences or symmetry, indicating a triclinic space group. Subsequent solution and refinement confirmed the correct choice to be $\bar{1}$.

Data were collected in the usual manner with use of a continuous θ–2θ scan technique. Data were reduced in the usual manner. The structure was solved by a combination of direct methods (MULTAN78) and Fourier techniques and refined by full-matrix least squares. Hydrogen atoms were visible in a Fourier phased on the non-hydrogen parameters and were included in the final cycles. Non-hydrogen atoms were assigned anisotropic thermal parameters while hydrogens were allowed to vary isotropically.

There is a molecule of hexane located at an inversion center in the lattice. No attempt was made to locate the hydrogen atoms associated with it.

Zr(OAr-2,6-*t*-Bu_2)$_2$(η^2-*t*-BuNCCH$_2$Ph)$_2$ (IId). A suitable sample was transferred to the goniostat with use of standard inert atmosphere handling techniques and cooled to −157 °C for characterization and data

(31) Huffman, J. C.; Lewis, L. N.; Caulton, K. G. *Inorg. Chem.* **1980**, *19*, 2755.

(32) Fanwick, P. L.; Ogilvy, A. K.; Rothwell, I. P. *Organometallics*, in press.

collection. A systematic search revealed a monoclinic lattice with systematic extinctions corresponding to space groups *Cc* or *C2/c*. The structure was solved in the non-centric space group *Cc* but transformed to the centric *C2/c* after examination of the resulting structure. All atoms, including hydrogens, were located and refined.

A final difference Fourier was featureless, the largest peak being 0.21 e/Å^3.

Hf(OAr-2,6-*t*-Bu$_2$)$_2$(η^2-PhNCCH$_3$)$_2$ (IIg). Details of the data collection and structure refinement has been given previously[32] and are summarized in Table XIII. The crystals were examined under deoxygenated Nujol and mounted in an appropriate sized glass capillary surrounded by epoxy resin. The hydrogen atom positions were calculated after several cycles of anisotropic refinement assuming idealized geometries and a carbon-hydrogen bond distance of 0.95 Å. For methyl groups, one hydrogen position was located in the difference Fourier map, this position idealized and the other two hydrogen positions calculated. The hydrogens were not refined.

Zr(OAr-^{2,6}-*t*-Bu$_2$)(η^2-*t*-BuNCCH$_2$Ph)$_3$ (VIa). A suitable sample was selected and transferred to the goniostat with use of standard inert atmosphere handling techniques and cooled to −155 °C for characterization and data collection. A systematic search of a limited hemisphere of reciprocal space revealed a set of reflections which exhibited no symmetry or systematic extinctions. The data were indexed as triclinic with the space group $P\bar{1}$.

The crystal structure was solved by locating the Zr atom by means of direct methods (Multan), and the remaining non-hydrogen atoms were located in a difference Fourier phased by the Zr atom. The hydrogen atoms were introduced in calculated positions ($B = B + 1$, C–H = 0.95 Å). The structure was refined by full-matrix least squares, using anisotropic thermal parameters on all non-hydrogen atoms. The hydrogen atoms were fixed.

A final difference Fourier was essentially featureless, the largest peak being 0.35 e/Å.

Ta(OAr-2,6-Me$_2$)$_2$(η^2-xyNCCH$_3$)$_2$(CH$_3$) (VIa). A suitable sample was cleaved from a larger crystal with use of standard inert atmosphere handling techniques and transferred to the goniostat where it was cooled to −160 °C for characterization and data collection. A systematic search of a limited hemisphere of reciprocal space revealed a set of diffraction maxima with no apparent symmetry or systematic absences and indicating the probable space group $P\bar{1}$. Subsequent solution and refinement confirmed the choice.

The structure was solved by a combination of direct methods (MULTAN78) and Fourier techniques and refined by full-matrix least squares. All hydrogen atoms were located and refined.

A final difference Fourier was featureless, the largest peak being 0.91 e/Å^3, located at the metal site.

Acknowledgment. We thank the Department of Energy (Pittsburgh Energy Technology Center; Grant DE-FG 22-85PC80909) and the National Science Foundation (Grant CHE-8612063) for support of this research. I.P.R. gratefully acknowledges the Camille and Dreyfus Foundation for the award of a Teacher Scholar Grant as well as the Alfred P. Sloan Foundation for the award of a Fellowship.

Supplementary Material Available: Tables of fractional coordinates of hydrogen atoms, anisotropic thermal parameters, and complete bond distances and angles (54 pages); listing of observed and calculated structure factors (94 pages). Ordering information is given on any current masthead page.

Palladium(I) π Radicals. Electrochemical Preparation and Study of Their Reaction Pathways

Gregg A. Lane,[†] William E. Geiger,*[†] and Neil G. Connelly[‡]

Contribution from the Department of Chemistry, University of Vermont, Burlington, Vermont 05405, and School of Chemistry, University of Bristol, Bristol BS8 1TS, England. *Received September 11, 1986*

Abstract: The reduction of a series of Pd(II) complexes has been studied by electrochemistry and spectroscopy. Neutral Pd(I) radicals may be obtained from the reduction of (η^5-C$_5$Ph$_5$)Pd(η^4-diolefin) cations, where diolefin = 1,5-cyclooctadiene, norbornadiene, or dibenzocyclooctatetraene. The one-electron processes are diffusion-controlled and highly reversible, yielding the first stable Pd(I) π radicals. The dibenzocyclooctatetraene derivative is isolable. These complexes undergo radical reaction with water, chlorinated hydrocarbons, and peroxides to give π,σ-Pd(II) complexes identical with those obtained by direct attack of nucleophiles on the starting Pd(II) cationic complexes. Reversible oxidation of (η^5-C$_5$Ph$_5$)Pd(η^4-diolefin) cations demonstrates the existence of formal Pd(III) complexes in these systems. The pentaphenylcyclopentadienyl ligand gives kinetic stabilization to both Pd(I) and Pd(III), compared to the unsubstituted cyclopentadienyl analogues.

The catalytic oxidation of olefins by Pd(II) is an important reaction, being the basis of the well-known Wacker industrial process, in which ethylene is oxidized to acetaldehyde.[1-3] Although a Pd π complex has not been isolated from the Wacker reaction mixture, it is generally agreed that the key step in the process is attack on a Pd–ethylene complex by a nucleophile, probably water, with accompanying $\pi-\sigma$ rearrangment of the coordinated olefin:[4-7] Eventually, the organic moiety is released,

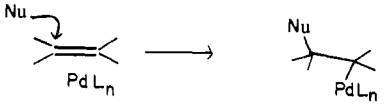

with formation of Pd metal, which is reoxidized to Pd(II) by excess Cu(II). Extensive studies of this and related reactions have failed to uncover any evidence that the intermediate oxidation state Pd(I) is involved in the reaction or, indeed, that any radical routes are important.[8]

(1) For leading references concerning the Wacker process, see: (a) Collman, J. P.; Hegedus, L. S. *Principles and Applications of Organotransition Metal Chemistry*; University Science Books: Mill Valley, CA, 1980; Dept. 5. (b) Heck, R. F. *Acc. Chem. Res.* **1979**, *12*, 146. (c) Henry, P. *Adv. Organomet. Chem.* **1975**, *13*, 363. (d) Davies, S. G. *Organotransition Metal Chemistry: Application to Organic Synthesis*; Pergamon: Oxford, 1982; pp 304–308.

(2) Eisenstein, O.; Hoffmann, R. *J. Am. Chem. Soc.* **1981**, *103*, 4308.

(3) Stille, J. K.; Hines, L. F.; Fries, R. W.; Wong, P. K.; James, D. E.; Lau, K. *Adv. Chem. Ser.* **1974**, *132*, 90.

(4) Sheldon, R. A.; Kochi, J. K. *Metal-Catalyzed Oxidation of Organic Compounds*; Academic: New York, 1981; pp 190–193.

(5) Backvall, J. E.; Akermark, B.; Ljunggren, S. O. *J. Am. Chem. Soc.* **1979**, *101*, 2411.

(6) Stille, J. K.; Divakaruni, R. *J. Organomet. Chem.* **1979**, *169*, 239.

(7) Stille, J. K.; Divakaruni, R. *J. Am. Chem. Soc.* **1978**, *100*, 1303.

(8) Kochi, J. K. *Organometallic Mechanisms and Catalysis*; Academic: New York, 1978; p 113.

0002-7863/87/1509-0402$01.50/0